Structural Engineering and Mechanics, *Vol. 62, No. 3 (2017) 325-344*
DOI: https://doi.org/10.12989/sem.2017.62.3.325

Influence of imperfectly bonded piezoelectric layer with irregularity on propagation of Love-type wave in a reinforced composite structure

Abhishek Kumar Singh[a], Mriganka Shekhar Chaki[*], Bristi Hazra[b] and Shruti Mahto[c]

Department of Applied Mathematics, Indian Institute of Technology (Indian School of Mines), Dhanbad, Jharkhand 826004, India

(Received August 21, 2016, Revised January 2, 2017, Accepted January 19, 2017)

Abstract. The present paper investigates the propagation of Love-type wave in a composite structure comprised of imperfectly bonded piezoelectric layer with lower fiber-reinforced half-space with rectangular shaped irregularity at the common interface. Closed-form expression of phase velocity of Love-type wave propagating in the composite structure has been deduced analytically for electrically open and short conditions. Some special cases of the problem have also been studied. It has been found that the obtained results are in well-agreement to the Classical Love wave equation. Significant effects of various parameters viz. irregularity parameter, flexibility imperfectness parameter and viscoelastic imperfectness parameter associated with complex common interface, dielectric constant and piezoelectric coefficient on phase velocity of Love-type wave has been reported. Numerical computations and graphical illustrations have been carried out to demonstrate the deduced results for various cases. Moreover, comparative study has been performed to unravel the effects of the presence of reinforcement and piezoelectricity in the composite structure and also to analyze the existence of irregularity and imperfectness at the common interface of composite structure in context of the present problem which serves as a salient feature of the present study.

Keywords: Love-type wave; reinforced composite; piezoelectric; imperfectness; irregularity; electrically open and short

1. Introduction

Electroelastic materials which exhibit electromechanical coupling experience mechanical deformations when placed in an electric field, become electrically polarized under mechanical loads. Piezoelectricity is a linear interaction between electrical and mechanical systems. By virtue of the intrinsic coupling effects between the electrical and the mechanical fields, piezoelectric materials have found extensive applications in smart devices such as electro-mechanical sensors, actuators and transducers. The brittleness in mechanical behavior is the inherent weakness of piezoelectric ceramics. In most of their applications, piezoelectric crystals, ceramics and composites are exposed to severe mechanical and electrical loading conditions, which may result in structural fracture or failure. The piezoelectric effect was discovered by Curie and Curie (1880). In dynamic applications involving production and detection of sound, generation of high voltages, electronic frequency generation, vibration suppression, microbalances, sensing, sonar, audio buzzers and air ultrasonic transducers these materials are found to be very effective. For the piezoelectric elements in the form of a thin plate, i.e. when the thickness of the piezoelectric material is much smaller than the wavelength of the elastic waves, the governing equations for the general three-dimension are given by Auld (1990), Tiersten (1969). Jakoby and Vellekoop (1969) discussed the basic properties of Love waves and their utilization in sensor devices.

Liu *et al*. (2001) investigated the effect of initial stress on the propagation behavior of Love waves in a layered piezoelectric structure. Li *et al*. (2004), Du *et al*. (2007) discussed Love wave propagation in FGPM layer. Qian *et al*. (2007) analyzed the propagation of transverse surface waves on a piezoelectric material carrying a functionally graded layer of finite thickness. Eskandari and Shojda (2008) elaborated Love wave propagation in functionally graded piezoelectric materials with quadratic variation.

Du *et al*. (2008) have discussed on propagation of Love waves in pre-stressed piezoelectric layered structures loaded with viscous liquid whereas Liu *et al*. (2008) analyzed Love wave propagation in layered piezoelectric/piezomagnetic structures. Pang *et al*. (2008) traced out reflection and refraction of plane waves at the interface between piezoelectric and piezomagnetic media. Piliposian and Danoyan (2009) examined the surface electro-elastic Love waves in a layered structure with a piezoelectric substrate and two isotropic layers. Later on, Liu and He (2010) studied the properties of Love waves in layered piezoelectric structures.

The study of the mechanical behavior of a fiber-reinforced material is of great importance in geomechanics and geo-engineering. Fiber-reinforced materials are a family of composite materials, where the polymer fibers are reinforced by highly oriented polymer fibers, derived from

∗Corresponding author, Ph.D. Student
E-mail: mriganka.chaki@gmail.com
[a]Ph.D.
E-mail: abhi.5700@gmail.com
[b]M.Sc. Student
E-mail: hazra.bristi@gmail.com
[c]Ph.D. Student and IT Analyst (TCS, Pune, India)
E-mail: ms.shrutimahto@gmail.com

http://www.techno-press.org/?journal=sem&subpage=8 ISSN: 1225-4568 (Print), 1598-6217 (Online)

the same fiber. Alumina or concrete is an example of fiber-reinforced material. Belfield *et al*. (1983) studied the stress in elastic plates reinforced with fibers lying in concentric circles. Hashin and Rosen (1964) investigated on the elastic moduli for fiber-reinforced materials. Singh (2006) analyzed the wave propagation in thermally conducting linear fiber-reinforced composite materials with one relaxation time

The above studies are based on the assumption that the layer is perfectly bonded to the substrate. However, due to aging of glue applied to two conjunct solids, microdefects, diffusion impurities, and other forms of damages, imperfect bonding often occurs in surface acoustic wave (SAW) devices. Schoenberg (1980) discussed the elastic wave behavior across linear slip interface. Termonia (1990) experimented on fibre coating as a means to compensate for poor adhesion in fibre-reinforced materials. Nagy (1992) gave the ultrasonic classification of imperfect interfaces. In the design and application of piezoelectric sensors, considering a possible imperfect interface is necessary. Chen and Lee (2004) discussed the exact solution of angle-ply piezoelectric laminates in cylindrical bending with interfacial imperfections. Otero (2012) studied the interfacial waves between two piezoelectric half-spaces with electro-mechanical imperfect interface.

Irregular boundaries on the elastic wave propagation have gained much in importance due to their closeness to natural environmental conditions. A lot of works has been discussed regarding the propagation of seismic waves concerning irregularity at an interface. Bhattacharya (1962) considered the irregularity in the thickness of the transversely isotropic crustal layer. Chattopadhyay *et al*. (2008) investigated propagation of SH waves in an irregular monoclinic crustal layer. Later on, Chattopadhyay *et al*. (2012) studied dispersion of horizontally polarized shear waves in an irregular non-homogeneous self-reinforced crustal layer over a semi-infinite self-reinforced medium. The propagation of magnetoelastic shear waves in an irregular self-reinforced layer was calibrated by Chattopadhyay and Singh (2012). Kaur *et al*. (2014) analyzed dynamic response of normal moving load on an irregular fiber-reinforced half-space. Lately, Singh *et al*. (2015) discussed the Love-type wave propagation in a piezoelectric structure with irregularity.

Recently, Peng and Feng (2015) studied the excitation and propagation of shear horizontal waves in a piezoelectric layer imperfectly bonded to a metal or elastic substrate. Kaur *et al*. (2016) discussed the influence of imperfectly bonded micropolar elastic half-space with non-homogeneous viscoelastic layer on propagation behavior of shear wave. To date, no study has been done on the propagation of Love waves in an imperfectly bonded piezoelectric layer lying over a fiber-reinforced half-space with an irregularity at the common interface.

In the present study, the dispersion relation for the Love-type wave propagating in a composite structure comprised of imperfectly bonded piezoelectric layer with lower fiber-reinforced half-space with rectangular shaped irregularity at the common interface has been obtained in closed-form for both electrically open and short conditions. Some special cases of the problem have also been studied and the obtained results are found to be in well-agreement to the Classical Love wave equation. To unravel the effects of various parameters viz. irregularity parameter, flexibility imperfectness parameter and viscoelastic imperfectness parameter associated with complex common interface, dielectric constant and piezoelectric coefficient on phase velocity of Love-type propagating in the composite structure, numerical computation and graphical illustration have been carried out. Moreover, comparative study has been performed to demonstrate the effects of irregularity and imperfectness at the common interface and the presence of reinforcement and piezoelectricity in the composite structure which leads to some significant results.

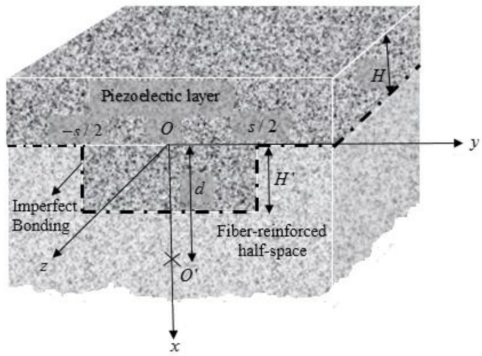

Fig. 1 Geometry of the problem

2. Formulation of the problem

We consider a composite structure constituted by imperfectly bonded piezoelectric layer of finite thickness H with a lower fiber-reinforced half space containing an irregularity at the common interface. Let us consider the co-ordinate system in such a way that y-axis is in direction of Love-type wave propagating along the interface between the layer and the lower semi-infinite medium and x-axis is pointing vertically downwards. We assume irregularity in the form of rectangle with span s and maximum depth H'. The origin is placed at the middle point of the span of the irregularity as shown in Fig. 1. The source of the disturbance is placed on positive-axis at a distance $d(>H')$ from the origin.

The equation of the common interface containing rectangular irregularity is defined as

$$x = \varepsilon h(y), \tag{1}$$

where

$$h(y) = \begin{cases} 0 & \text{for } |y| > \dfrac{s}{2}, \\ s & \text{for } |y| \le \dfrac{s}{2}, \end{cases}$$

where $\varepsilon=H'/s<<1$ is a small positive number called perturbation parameter. Assumption $\varepsilon<<1$ finds its practical implication in those fabricated composite structure where the depth H' of the irregularity is too small with respect to the span s of the irregularity. The mechanical displacement components for the upper piezoelectric layer and lower fiber-reinforced half space in x,y and z directions are assumed to be (u_1,v_1,w_1) and (u_2,v_2,w_2) respectively. For the Love-type wave propagating in the y-direction and causing displacement in z-direction only, we take

$$\left.\begin{aligned} u_1 = 0, \quad v_1 = 0, \quad w_1 = w_1(x,y,t), \\ u_2 = 0, \quad v_2 = 0, \quad w_2 = w_2(x,y,t). \end{aligned}\right\} \tag{2}$$

Let us assume the electric potential function for the upper imperfectly bonded irregular piezoelectric layer as

$$\phi = \phi(x,y,t). \tag{3}$$

3. Governing equation of motion for upper irregular imperfectly bonded piezoelectric layer

The equation of motion for upper imperfectly bonded irregular piezoelectric layer is given by

$$\left.\begin{aligned} \frac{\partial \sigma_{xx}}{\partial x} + \frac{\partial \sigma_{xy}}{\partial y} + \frac{\partial \sigma_{xz}}{\partial z} = \rho_1 \frac{\partial^2 u_1}{\partial t^2}, \\ \frac{\partial \sigma_{yx}}{\partial x} + \frac{\partial \sigma_{yy}}{\partial y} + \frac{\partial \sigma_{yz}}{\partial z} = \rho_1 \frac{\partial^2 v_1}{\partial t^2}, \\ \frac{\partial \sigma_{zx}}{\partial x} + \frac{\partial \sigma_{zy}}{\partial y} + \frac{\partial \sigma_{zz}}{\partial z} = \rho_1 \frac{\partial^2 w_1}{\partial t^2}, \end{aligned}\right\} \tag{4}$$

with

$$D_{i,j} = 0, \tag{5}$$

where i,j=1,2,3; ρ_1 is the mass density of upper piezoelectric layer; D_i denote the electric displacement in the i th-direction respectively; and σ_{ij} is the stress tensor.

The constitutive equations for a transversely isotropic piezoelectric medium with z-axis being the symmetric axis of the material is given by

$$\left.\begin{aligned} \sigma_x &= c_{11}S_x + c_{12}S_y + c_{13}S_z - e_{31}E_z, \\ \sigma_y &= c_{12}S_x + c_{11}S_y + c_{13}S_z - e_{31}E_z, \\ \sigma_z &= c_{13}S_x + c_{13}S_y + c_{33}S_z - e_{33}E_z, \\ \sigma_{yz} &= c_{44}S_{yz} - e_{15}E_y, \\ \sigma_{zx} &= c_{44}S_{zx} - e_{15}E_x, \\ \sigma_{xy} &= \frac{1}{2}(c_{11} - c_{12})S_{xy}, \\ D_x &= e_{15}S_{zx} + \varepsilon_{11}E_x, \\ D_y &= e_{15}S_{yz} + \varepsilon_{11}E_y, \\ D_z &= e_{31}S_x + e_{31}S_y + e_{33}S_z + \varepsilon_{33}E_z, \end{aligned}\right\} \tag{6}$$

where c_{11},c_{12},c_{13},c_{33} and c_{44} are elastic constant; e_{15}, e_{31} and e_{33} are piezoelectric constants; and ε_{11} and ε_{33} are dielectric constants of the upper irregular imperfectly bonded piezoelectric layer.

The mechanical displacement components together with the strain components gives the relations as

$$S_x = \frac{\partial u_1}{\partial x}, S_y = \frac{\partial v_1}{\partial y}, S_z = \frac{\partial w_1}{\partial z}, S_{yz} = \frac{\partial w_1}{\partial y} + \frac{\partial v_1}{\partial z}, S_{zx} = \frac{\partial u_1}{\partial z} + \frac{\partial w_1}{\partial x}$$
$$\text{and } S_{xy} = \frac{\partial u_1}{\partial y} + \frac{\partial v_1}{\partial x}. \tag{7}$$

The relation between electric intensity and the electrical potential is given by

$$E_x = -\frac{\partial \phi}{\partial x}, E_y = -\frac{\partial \phi}{\partial y} \text{ and } E_z = -\frac{\partial \phi}{\partial z}. \tag{8}$$

In view of Eq.(2), Eqs.(7) and (8) result in

$$S_x = 0, S_y = 0, S_z = 0, S_{xy} = 0, S_{yz} = \frac{\partial w_1}{\partial y}, S_{zx} = \frac{\partial w_1}{\partial x}, \tag{9}$$

and

$$E_x = -\frac{\partial \phi}{\partial x}, E_y = -\frac{\partial \phi}{\partial y}, E_z = 0 \tag{10}$$

Using Eqs. (9) and (10), Eq. (6) yields

$$\left.\begin{aligned} &\sigma_x = 0, \sigma_y = 0, \sigma_z = 0, \sigma_{xy} = 0, \\ &\sigma_{yz} = c_{44}\frac{\partial w_1}{\partial y} + e_{15}\frac{\partial \phi}{\partial y}, \sigma_{zx} = c_{44}\frac{\partial w_1}{\partial x} + e_{15}\frac{\partial \phi}{\partial x}, \\ &D_z = 0, D_x = e_{15}\frac{\partial w_1}{\partial x} - \varepsilon_{11}\frac{\partial \phi}{\partial x} \\ &\text{and } D_y = e_{15}\frac{\partial w_1}{\partial y} - \varepsilon_{11}\frac{\partial \phi}{\partial y}. \end{aligned}\right. \tag{11}$$

Now, using Eq.(2) in Eqs.(4) and (5),we obtain

$$\frac{\partial \sigma_{zx}}{\partial x} + \frac{\partial \sigma_{yz}}{\partial y} = \rho_1 \frac{\partial^2 w_1}{\partial t^2} \tag{12}$$

and

$$\frac{\partial D_x}{\partial x} + \frac{\partial D_y}{\partial y} = 0. \tag{13}$$

With the help of Eq. (11) in Eqs. (12) and (13), we have the governing equations for propagation of Love- type wave in the upper imperfectly bonded piezoelectric layer with irregularity as

$$\left.\begin{aligned} c_{44}\nabla^2 w_1 + e_{15}\nabla^2 \phi = \rho_1 \ddot{w}_1, \\ e_{15}\nabla^2 w_1 - \varepsilon_{11}\nabla^2 \phi = 0, \end{aligned}\right\} \tag{14}$$

where ∇^2 is two dimensional Laplacian operator.

Now the above equation can be rewritten as

$$\left.\begin{aligned} \nabla^2 \omega_1 - \frac{1}{c_1^2}\ddot{\omega}_1 = 0, \\ \nabla^2 \phi - \frac{1}{c_1^2}\left(\frac{e_{15}}{\varepsilon_{11}}\right)\ddot{\omega}_1 = 0, \end{aligned}\right\} \tag{15}$$

where $c_1 = \sqrt{\frac{\overline{c_{44}}}{\rho_1}}, \overline{c_{44}} = \left(c_{44} + \frac{e_{15}^2}{\varepsilon_{11}}\right)$; c_1 and c_2 are the bulk shear wave velocity in the upper irregular imperfectly bonded piezoelectric layer.

Then, Eq. (15) can be written as

$$\left.\begin{aligned} \frac{\partial^2 w_1}{\partial x^2}+\frac{\partial^2 w_1}{\partial y^2}-\frac{1}{c_1^2}\frac{\partial^2 w_1}{\partial t^2}=0 \\ \frac{\partial^2 \phi}{\partial x^2}+\frac{\partial^2 \phi}{\partial y^2}-\frac{1}{c_1^2}\frac{e_{15}}{\varepsilon_{11}}\frac{\partial^2 w_1}{\partial t^2}=0 \end{aligned}\right\}. \tag{16}$$

4. Governing equation of motion for the lower fiber-reinforced half space

The constitutive equation for fiber-reinforced elastic medium (Belfield *et al*. 1983) is

$$\begin{aligned} \tau_{ij} &= \lambda e_{kk}\delta_{ij}+2\mu_T e_{ij}+\alpha(a_k a_m e_{km}\delta_{ij}+e_{kk}a_i a_j)+2(\mu_L-\mu_T) \\ &\quad\times(a_i a_k e_{kj}+a_j a_k e_{ki})+\beta a_k a_m e_{km} a_i a_j,\ (i,j,k,m=1,2,3) \end{aligned} \tag{17}$$

where τ_{ij} are components of stress, $e_{ij}(=\frac{1}{2}(u_{i,j}+u_{j,i}))$ are components of infinitesimal strain, δ_{ij} is kronecker delta, $\vec{a}=(a_1,a_2,a_3)$ is the direction of reinforcement such that $a_1^2+a_2^2+a_3^2=1$ and λ, μ_L, μ_T, α and β are elastic constants; μ_T is the transverse shear modulus across the preferred direction whereas μ_L is the longitudinal shear modulus across the preferred direction.

In view of Eq. (2), the governing equation of motion for small elastic disturbance in the lower fiber-reinforced half space is given by

$$\frac{\partial \tau_{zx}}{\partial x}+\frac{\partial \tau_{yz}}{\partial y}=\rho_2\frac{\partial^2 w_2}{\partial t^2}, \tag{18}$$

where ρ_2 is the material density of the fiber-reinforced half-space,and

$$\left.\begin{aligned} \tau_{zx} &= \mu_T\frac{\partial w_2}{\partial x}+(\mu_L-\mu_T)a_1\left(a_1\frac{\partial w_2}{\partial x}+a_2\frac{\partial w_2}{\partial y}\right), \\ \tau_{zy} &= \mu_T\frac{\partial w_2}{\partial y}+(\mu_L-\mu_T)a_2\left(a_1\frac{\partial w_2}{\partial x}+a_2\frac{\partial w_2}{\partial y}\right). \end{aligned}\right\} \tag{19}$$

Now using Eq.(19), Eq.(18) leads to

$$P\frac{\partial^2 w_2}{\partial x^2}+Q\frac{\partial^2 w_2}{\partial y^2}+R\frac{\partial^2 w_2}{\partial x\partial y}=\frac{1}{\beta_2^2}\frac{\partial^2 w_2}{\partial t^2}, \tag{20}$$

where

$$P=1+(\frac{\mu_L}{\mu_T}-1)a_2^2,\ Q=1+(\frac{\mu_L}{\mu_T}-1)a_1^2,\ R=2a_1a_2(\frac{\mu_L}{\mu_T}-1)$$

and $\beta_2=\sqrt{\frac{\mu_T}{\rho_2}}$.

5. Boundary conditions

For the propagation of Love-type wave in composite structure comprised of piezoelectric layer imperfectly bonded to a lower fiber-reinforced half-space containing irregularity at the common interface, two types of electrical boundary conditions, i.e., electrically open and electrically short conditions, have been considered in this study. The boundary conditions (mechanical and electrical) are as follows:

(i) The electrical boundary conditions at free surface i.e., at $x=-H$ are as follows:

(a) The electrical open condition at $x=-H$ is

$$D_x(-H,y)=0, \tag{21}$$

(b) The electrical short condition at $x=-H$ is

$$\phi(-H,y)=0, \tag{22}$$

(ii) The mechanical traction free condition at $x=-H$ is

$$\sigma_{zx}(-H,y)=0, \tag{23}$$

(iii) Conditions at the imperfectly bonded irregular interface i.e., at $x=\varepsilon h(y)$ are

$$\text{(a)}\quad \tau_{zx}-\varepsilon h'(y)\tau_{yz}=\sigma\left(w_1-w_2\right), \tag{24}$$

$$\text{(b)}\quad \phi=0, \tag{25}$$

$$\text{(c)}\quad \sigma_{zx}-\varepsilon h'(y)\sigma_{yz}=\tau_{zx}-\varepsilon h'(y)\tau_{yz}, \tag{26}$$

where σ is imperfectness parameter of the common interface.

Eqs. (16), (20) and (21)-(26) presents the complete mathematical model for the problem.

6. Solution of the problem

We assume the solutions of the Eqs.(16) and (20) as

$$w_r=W_r(x,y)e^{i\omega t} \text{ and } \phi_r=\varphi_r(x,y)e^{i\omega t};(r=1,2) \tag{27}$$

where $\omega(=kc$, with k being the wave number and c being the phase velocity) is circular frequency of Love-type wave.

In light of (27), Eqs. (16) and (20) reduce to

$$\left.\begin{aligned} \frac{\partial^2 W_1}{\partial x^2}+\frac{\partial^2 W_1}{\partial y^2}+\frac{\omega^2}{c_1^2}W_1=0, \\ \frac{\partial^2 \varphi}{\partial x^2}+\frac{\partial^2 \varphi}{\partial y^2}+\frac{\omega^2}{c_1^2}\frac{e_{15}}{\varepsilon_{11}}W_1=0, \end{aligned}\right\} \tag{28}$$

and

$$P\frac{\partial^2 W_2}{\partial x^2}+Q\frac{\partial^2 W_2}{\partial y^2}+R\frac{\partial^2 W_2}{\partial x\partial y}+\frac{\omega^2}{\beta_2^2}\frac{\partial^2 W_2}{\partial t^2}=0. \tag{29}$$

Defining the Fourier transforms $\bar{W}_r(x,\eta)$ and $\bar{\varphi}(x,\eta)$ of $W_r(x,y)$ and $\varphi(x,y)$ respectively $(r=1,2)$ as

$$\bar{W}_r(x,\eta)=\int_{-\infty}^{\infty}W_r(x,y)e^{i\eta y}dy,$$

$$\bar{\varphi}(x,\eta)=\int_{-\infty}^{\infty}\varphi(x,y)e^{i\eta y}dy,$$

with the inverse Fourier Transforms as

$$W_r(x,y)=\frac{1}{2\pi}\int_{-\infty}^{\infty}\overline{W}_r(x,\eta)e^{-i\eta y}d\eta,$$
$$\varphi(x,y)=\frac{1}{2\pi}\int_{-\infty}^{\infty}\overline{\varphi}(x,\eta)e^{-i\eta y}d\eta,$$

where η is a transform parameter.

Taking Fourier transforms of Eqs. (28) and (29), we get

$$\left.\begin{aligned}&\frac{d^2\overline{W}_1}{dx^2}+P_1^2\overline{W}_1=0,\\&\frac{d^2\overline{\phi}}{dx^2}-\eta^2\overline{\phi}+\frac{\omega^2}{c_1^2}\frac{e_{15}}{\varepsilon_{11}}\overline{W}_1=0,\end{aligned}\right\}\tag{30}$$

and

$$P\frac{\partial^2\overline{W_2}}{\partial x^2}-i\eta R\frac{\partial\overline{W_2}}{\partial x}+\left(\frac{\omega^2}{\beta_2^2}-Q\eta^2\right)\overline{W_2}=0,\tag{31}$$

where $P_1=\sqrt{\dfrac{\omega^2}{c_1^2}-\eta^2}$.

The solution of Eq. (30) may be expressed as

$$\left.\begin{aligned}&\overline{W_1}(x,\eta)=AcosP_1x+BsinP_1x,\\&\overline{\varphi}(x,\eta)=Ce^{-\eta x}+De^{\eta x}+\frac{e_{15}}{\varepsilon_{11}}(AcosP_1x+BsinP_1x)\end{aligned}\right\}\tag{32}$$

and the solution of Eq. (31) may be expressed as

$$\overline{W_2}(x,\eta)=Ee^{-P_2x},\tag{33}$$

where $P_2=\dfrac{i\eta R}{2P}+\eta\sqrt{\dfrac{s_2^2}{P}-\dfrac{R^2}{4P^2}}$ and $s_2=\sqrt{Q\eta^2-\dfrac{\omega^2}{\beta_2^2}}$.

Therefore, mechanical displacement and electric potential function in upper piezoelectric layer are

$$\left.\begin{aligned}&W_1(x,y)=\frac{1}{2\pi}\int_{-\infty}^{\infty}(AcosP_1x+BsinP_1x)e^{-i\eta y}d\eta\\&\varphi(x,y)=\frac{1}{2\pi}\int_{-\infty}^{\infty}\left[Ce^{-\eta x}+De^{\eta x}+\frac{e_{15}}{\varepsilon_{11}}(AcosP_1x+BsinP_1x)\right]e^{-i\eta y}d\eta\end{aligned}\right\}\tag{34}$$

and the mechanical displacement in lower fiber-reinforced half space is

$$W_2=\frac{1}{2\pi}\int_{-\infty}^{\infty}\left[Ee^{-P_2x}+\frac{2}{P_2}e^{P_2x}e^{-P_2d}\right]e^{-i\eta y}d\eta,\tag{35}$$

where the second term in the integrand of W_2 is introduced due to the presence of source in the lower fiber-reinforced half-space.

Since boundary is not uniform, the terms A,B,C,D and E appearing in Eqs. (34) and (35) are also functions of ε. These terms can be expanded in ascending powers of ε. Since ε is small, therefore retaining the terms up to the first order of ε, we can approximate A,B,C,D and E as follows:

$$A\cong A_0+A_1\varepsilon,B\cong B_0+B_1\varepsilon,C\cong C_0+C_1\varepsilon,$$
$$D\cong D_0+D_1\varepsilon,E\cong E_0+E_1\varepsilon.$$

For the small ε, we may further use the following approximations:

$$e^{\pm v\varepsilon h}\cong 1\pm v\varepsilon h, cos(v\varepsilon h)\cong 1, sin(v\varepsilon h)\cong v\varepsilon h,$$

where v is any quantity.

From boundary condition (21), (22) and (23), we have

$$\varepsilon_{11}\left[(C_0+C_1\varepsilon)\eta e^{\eta H}-(D_0+D_1\varepsilon)\eta e^{-\eta H}\right]=0,\tag{36}$$

$$\begin{aligned}&(C_0+C_1\varepsilon)e^{\eta H}-(D_0+D_1\varepsilon)e^{-\eta H}\\&\quad+\frac{e_{15}}{\varepsilon_{11}}\left[(A_0+A_1\varepsilon)cosP_1H-(B_0+B_1\varepsilon)sinP_1H\right]=0,\end{aligned}\tag{37}$$

and

$$\begin{aligned}&c_{44}[(A_0+A_1\varepsilon)P_1sinP_1+(B_0+B_1\varepsilon)P_1cosP_1H]\\&\quad+e_{15}\big[-(C_0+C_1\varepsilon)\eta e^{\eta H}-(D_0+D_1\varepsilon)\eta e^{-\eta H}\\&\quad+\frac{e_{15}}{\varepsilon_{11}}(A_0+A_1\varepsilon)P_1sinP_1H+(B_0+B_1\varepsilon)P_1cosP_1H\big]=0.\end{aligned}\tag{38}$$

Using boundary conditions (24), we get

$$\begin{aligned}&\int_{-\infty}^{\infty}\{\mu_T\big[-P_2(E_0+E_1\varepsilon)(1-P_2\varepsilon h(y))+2(1+P_2\varepsilon h(y))e^{-P_2d}\big]\\&+(\mu_L-\mu_T)a_1\big(a_1\big[-P_2(E_0+E_1\varepsilon)(1-P_2\varepsilon h(y))\\&+2(1+P_2\varepsilon h(y))e^{-P_2d}\big]-i\eta a_2\big[(E_0+E_1\varepsilon)(1-P_2\varepsilon h(y))\\&+\frac{2}{P_2}(1+P_2\varepsilon h(y))e^{-P_2d}\big]\big)\}e^{-i\eta y}d\eta-\varepsilon\int_{-\infty}^{\infty}\big[\mu_T\big[(E_0+E_1\varepsilon)\\&\times(1-P_2\varepsilon h(y))+\frac{2}{P_2}(1+P_2\varepsilon h(y))e^{-P_2d}\big](-i\eta)+(\mu_L-\mu_T)a_2\\&\times\big(a_1\big[-P_2(E_0+E_1\varepsilon)(1-P_2\varepsilon h(y))+2(1+P_2\varepsilon h(y))e^{-P_2d}\big]\\&-i\eta a_2\big[(E_0+E_1\varepsilon)(1-P_2\varepsilon h(y))+\frac{2}{P_2}(1+P_2\varepsilon h(y))e^{-P_2d}\big]\big)\big]\\&\times h'(y)e^{-i\eta y}d\eta=\sigma\int_{-\infty}^{\infty}\big[(E_0+E_1\varepsilon)(1-P_2\varepsilon h(y))+\frac{2}{P_2}(1+P_2\varepsilon h(y))\\&\times e^{-P_2d}-\{(A_0+A_1\varepsilon)-(B_0+B_1\varepsilon)(P_1\varepsilon h(y))\}\big]e^{-i\eta y}d\eta.\end{aligned}\tag{39}$$

Now, defining the Fourier transform of $h(y)$ as

$$\overline{h}(\lambda)=\int_{-\infty}^{\infty}h(y)e^{i\lambda y}dy,\tag{40}$$

with the inverse Fourier transform as

$$h(y)=\frac{1}{2\pi}\int_{-\infty}^{\infty}\overline{h}(\lambda)e^{-i\lambda y}d\lambda.\tag{41}$$

Therefore, we have

$$h'(y)=\frac{-i}{2\pi}\int_{-\infty}^{\infty}\lambda\overline{h}(\lambda)e^{-i\lambda y}d\lambda.\tag{42}$$

With the help of the Eqs. (41) and (42), Eq. (39) becomes

$$\begin{aligned}&\frac{\varepsilon}{2\pi}\int_{-\infty}^{\infty}\big[\int_{-\infty}^{\infty}\big[\mu_TE_0P_2^2+2\mu_TP_2e^{-P_2d}+(\mu_L-\mu_T)(a_1^2P_2^2E_0)\\&+(\mu_L-\mu_T)(2a_1^2P_2e^{-P_2d})+(\mu_L-\mu_T)(-i\eta)(-a_1a_2E_0P_2\\&+2a_1a_2e^{-P_2d})+i\lambda\{\frac{2\mu_T}{P_2}e^{-P_2d}(-i\eta)+(\mu_L-\mu_T)a_2\big[a_1(-P_2E_0\end{aligned}$$

$$
\begin{aligned}
&+2e^{-P_2 d})-i\eta a_2(E_0+\frac{2}{P_2}e^{-P_2 d})\big]+\mu_T E_0(-i\eta)\big\} \\
&+\sigma\big\{P_2E_0-2e^{-P_2 d}+B_0P_1\big\}\big]\bar{h}(\lambda)e^{-i(\eta+\lambda)y}d\eta\big]d\lambda \qquad (43)\\
&=\int_{-\infty}^{\infty}\big\{\mu_T P_2E_0+\mu_T P_2E_1\varepsilon-2\mu_T e^{-P_2 d} \\
&\quad -(\mu_L-\mu_T)a_1\big[-a_1P_2E_0-a_1P_2E_1\varepsilon+2a_1e^{-P_2 d} \\
&\quad +(-i\eta)a_2\left(E_0+E_1\varepsilon\right)-i\eta a_2\frac{2}{P_2}e^{-P_2 d}\big] \\
&\quad +\sigma\big[E_0+E_1\varepsilon+\frac{2}{P_2}e^{-P_2 d}-(A_0+A_1\varepsilon)\big]\big\}e^{-i\eta y}d\eta.
\end{aligned}
$$

Putting $\eta+\lambda=k$ for the inner integral in the left-hand side of Eq. (43), so that λ may be treated as a constant. Therefore $d\eta=dk$ and finally replacing η by k in the right hand side of Eq. (43) and using Eq. (40), we get

$$
\begin{aligned}
&-\sigma(E_0+E_1\varepsilon)-\frac{2}{P_2}\sigma e^{-P_2 d}+A_0\sigma+A_1\sigma\varepsilon-\mu_T E_0P_2 \\
&-E_1\varepsilon P_2\mu_T+2\mu_T e^{-P_2 d}+(\mu_L-\mu_T)a_1\big[-a_1E_0P_2-a_1E_1\varepsilon P_2 \qquad (44)\\
&+2e^{-P_2 d}a_1-ika_2E_0-ika_2E_1\varepsilon-ika_2\frac{2}{P_2}e^{-P_2 d}\big]=\varepsilon R_1(k)
\end{aligned}
$$

where

$$
\begin{aligned}
R_1(k)=&\frac{1}{2\pi}\int_{-\infty}^{\infty}\big[-P_2E_0\sigma+2e^{-P_2 d}\sigma-B_0P_1\sigma-\mu_T E_0P_2^2-2P_2\mu_T e^{-P_2 d} \\
&-(\mu_L-\mu_T)a_1\big[a_1E_0P_2^2+2a_1e^{-P_2 d}P_2+ika_2E_0P_2-2ika_2e^{-P_2 d}\big] \\
&-i\lambda\big\{\big(\mu_T E_0+\frac{2}{P_2}\mu_T e^{-P_2 d}\big)(-ik)+(\mu_L-\mu_T)a_2\big[a_1(-P_2E_0+2e^{-P_2 d}) \\
&-ika_2\big(E_0+\frac{2}{P_2}e^{-P_2 d}\big)\big]\big\}\big]^{\eta=k-\lambda}\bar{h}(\lambda)d\lambda.
\end{aligned} \qquad (45)
$$

Proceeding in the similar manner which is adopted to result in Eq. (44), from the boundary conditions (25) and (26) with the help of Eqs. (40) and (41), respectively yields

$$
C_0+C_1\varepsilon+D_0+D_1\varepsilon+(A_0+A_1\varepsilon)\frac{e_{15}}{\varepsilon_{11}}=\varepsilon R_2(k), \qquad (46)
$$

and

$$
\begin{aligned}
&-c_{44}B_0P_1-c_{44}B_1\varepsilon P_1-e_{15}[-kC_0-kC_1\varepsilon+D_0k+D_1\varepsilon k \\
&+\frac{e_{15}}{\varepsilon_{11}}(B_0P_1+B_1P_1\varepsilon)+\mu_T\left(-P_2E_0-P_2E_1\varepsilon+2e^{-P_2 d}\right) \\
&\quad +(\mu_L-\mu_T)a_1\big[a_1\left(-P_2E_0-P_2E_1\varepsilon+2e^{-P_2 d}\right) \qquad (47)\\
&\qquad -ika_2\big(E_0+E_1\varepsilon+\frac{2}{P_2}e^{-P_2 d}\big)\big]=\varepsilon R_3(k),
\end{aligned}
$$

where the newly introduced symbols appearing in Eqs. (46) and (47) are as

$$
R_2(k)=\frac{1}{2\pi}\int_{-\infty}^{\infty}\left[C_0k-D_0k-\frac{e_{15}}{\varepsilon_{11}}(B_0P_1)\right]^{\eta=k-\lambda}\bar{h}(\lambda)d\lambda, \qquad (48)
$$

$$
\begin{aligned}
R_3(k)=&\frac{1}{2\pi}\int_{-\infty}^{\infty}\big[-c_{44}A_0P_1^2+e_{15}\left(k^2C_0+D_0k^2+\frac{e_{15}}{\varepsilon_{11}}(-A_0P_1^2)\right) \\
&-\mu_T P_2^2E_0-\mu_T 2e^{-P_2 d}P_2-(\mu_L-\mu_T)a_1\big[a_1(P_2^2E_0+2e^{-P_2 d}P_2) \\
&-ika_2(-P_2E_0+2e^{-P_2 d})\big]+i\lambda\big\{(c_{44}A_0)(-ik) \qquad (49)\\
&+e_{15}[C_0+D_0+\frac{e_{15}}{\varepsilon_{11}}A_0(-ik)]-\big\{(-i\eta)(\mu_T E_0+\frac{2}{P_2}\mu_T e^{-P_2 d}) \\
&+(\mu_L-\mu_T)a_2[a_1(-P_2E_0+2e^{-P_2}) \\
&-i\eta a_2(E_0+\frac{2}{P_2}e^{-P_2 d})]\big\}\big\}\big]^{\eta=k-\lambda}\bar{h}(\lambda)d\lambda.
\end{aligned}
$$

7. Dispersion equation for electrically open case

Eqs. (21) and (23)-(26) together constitute the required boundary conditions for electrically open case.

Equating the absolute terms (i.e., terms not containing ε) and the coefficient of ε from Eqs. (36), (38), (44), (46) and (47), we obtain the following:

$$
\begin{aligned}
&C_0^0e^{kH}-D_0^0e^{-kH}=0, \\
&C_1^0e^{kH}-D_1^0e^{-kH}=0, \\
&\overline{C_{44}}[A_0^0P_1sinP_1H+B_0^0P_1cosP_1H]=0, \\
&\overline{C_{44}}[A_1^0P_1sinP_1H+B_1^0P_1cosP_1H]=0, \\
&-\sigma E_0^0-\frac{2}{P_2}\sigma e^{-P_2 d}+A_0^0\sigma-\mu_T E_0^0P_2+2\mu_T e^{-P_2 d} \\
&+(\mu_L-\mu_T)a_1\big[(-a_1E_0^0P_2+2e^{-P_2 d}a_1)-ika_2E_0^0-ika_2\frac{2}{P_2}e^{-P_2 d}\big]=0, \\
&-\sigma E_1^0+A_1^0\sigma-\mu_T E_1^0P_2 \\
&\qquad +(\mu_L-\mu_T)a_1[(-a_1E_1^0P_2-ika_2E_1^0]=R_1^0(k), \\
&C_0^0+D_0^0+A_0^0\frac{e_{15}}{\varepsilon_{11}}=0, \\
&C_1^0+D_1^0+A_1^0\frac{e_{15}}{\varepsilon_{11}}=R_2^0(k), \\
&-C_{44}B_0^0P_1-e_{15}\left[-kC_0^0+D_0^0k+\frac{e_{15}}{\varepsilon_{11}}(B_0^0P_1)\right]+\mu_T\left[-P_2E_0^0+2e^{-P_2 d}\right] \\
&\quad +(\mu_L-\mu_T)a_1\left[a_1\left(-P_2E_0^0+2e^{-P_2 d}\right)-ika_2\left(E_0^0+\frac{2}{P_2}e^{-P_2 d}\right)\right]=0,
\end{aligned}
$$

and

$$
\begin{aligned}
&-C_{44}B_1^0P_1-e_{15}\left[-kC_1^0+D_1^0k+\frac{e_{15}}{\varepsilon_{11}}(B_1^0P_1)\right]+\mu_T(-P_2E_1^0) \\
&\qquad +(\mu_L-\mu_T)a_1\left[a_1(-P_2E_1^0)-ika_2(E_1^0)\right]=R_3^0(k).
\end{aligned}
$$

On solving the above equations, we may obtain the expressions of ten unknowns viz. A_0^0, B_0^0, C_0^0, D_0^0, E_0^0, A_1^0, B_1^0, C_1^0, D_1^0 and E_1^0 which are referred in appendix A where the superscript " 0 " corresponds to the electrically open case.

Therefore, in light of above obtained values, the mechanical displacement in the upper irregular imperfectly bonded piezoelectric layer for electrically open case may be written with the help of Eq. (34) as

$$W_1^0 = \frac{1}{2\pi}\int_{-\infty}^{\infty}\frac{-4e^{-P_2 d}\sigma\varepsilon_{11}(1+e^{2kH})(\mu_T+(\mu_L-\mu_T)a_1^2)}{E^0(k)}$$
$$\left[1-\frac{\varepsilon\left[R_3^0(k)(\sigma+\xi)-\left(\frac{1-e^{2kH}}{1+e^{2kH}}\right)ke_{15}R_2^0(k)(\sigma+\xi)-R_1^0(k)\xi\right]e^{P_2 d}}{4[\mu_T+(\mu_L-\mu_T)a_1^2]\sigma}\right]$$
$$\times(\cos P_1 x-\tan P_1 H\sin P_1 x)e^{-iky}dk, \tag{50}$$

where $E^0(k)$ and ξ are provided in Appendix A.

Now, using Eq. (1) and Eq. (40), we get

$$\bar{h}(\lambda)=\frac{2s}{\lambda}\sin\left(\frac{\lambda s}{2}\right). \tag{51}$$

Using Eqs. (45), (48), (49) and (51),we get

$$R_3^0(k)(\sigma+\xi)-\left(\frac{1-e^{2kH}}{1+e^{2kH}}\right)ke_{15}R_2^0(k)(\sigma+\xi)-R_1^0(k)\xi$$
$$=\frac{s}{\pi}\int_{-\infty}^{\infty}[\psi^0(k-\lambda)+\psi^0(k+\lambda)]\frac{1}{\lambda}\sin\left(\frac{\lambda s}{2}\right)d\lambda, \tag{52}$$

where

$$\psi^0(k-\lambda)=[A_2+A_3+A_4]^{\eta=k-\lambda},$$

where, the value of A_2,A_3 and A_4 are defined in appendix A. The argument of $\psi^0(k-\lambda)$ is due to $\eta+\lambda=k$.

Now, using asymptotic formulas indicated by willis (1948) and Tranter (1966), we have

$$\int_{-\infty}^{\infty}[\psi^0(k-\lambda)+\psi^0(k+\lambda)]\frac{1}{\lambda}\sin\left(\frac{\lambda s}{2}\right)d\lambda\cong\frac{\pi}{2}2\psi^0(k)=\pi\psi^0(k). \tag{53}$$

Now, using Eq.(53) in Eq.(52), we obtain

$$R_3^0(k)(\sigma+\xi)-\left(\frac{1-e^{2kH}}{1+e^{2kH}}\right)ke_{15}R_2^0(k)(\sigma+\xi)-R_1^0(k)\xi$$
$$=\frac{s}{\pi}\pi\psi^0(k)=s\psi^0(k)=\frac{H'}{\varepsilon}\psi^0(k). \tag{54}$$

With the help of Eq. (54), Eq. (50) gives the required mechanical displacement of the irregular imperfectly bonded piezoelectric layer as

$$W_1^0=\frac{1}{2\pi}\int_{-\infty}^{\infty}\frac{-4e^{-P_2 d}\sigma\varepsilon_{11}(1+e^{2kH})(\mu_T+(\mu_L-\mu_T)a_1^2)}{E^0(k)\left[1+\frac{H'\psi^0(k)}{4[\mu_T+(\mu_L-\mu_T)a_1^2]\sigma}\right]}$$
$$\times(\cos P_1 x-\tan P_1 H\sin P_1 x)e^{-iky}dk. \tag{55}$$

The value of this integral depends upon the contribution of poles of the integrand. In order to find the pole, we calculate the roots of the following equation

$$E^0(k)\left[1+\frac{H'\psi^0(k)}{4[\mu_T+(\mu_L-\mu_T)a_1^2]\sigma}\right]=0. \tag{56}$$

Now, since $\Gamma=\frac{k\mu_T}{\sigma}$ is a non-dimensional number that describes how effectively the sensitive layer and the half-space are bonded and Γ=0 corresponding to the perfect bonding of layer with half-space. To take viscoelasticity of the imperfect interface into account, we use a complex interface stiffness i.e., $\sigma=\sigma_1+i\sigma_2$, where both σ_1 and σ_2 are real. we may write

$$\Gamma=\Gamma_1-i\Gamma_2=\frac{\mu_T k}{\sigma_1+i\sigma_2}=\frac{\mu_T k}{|\sigma|^2}(\sigma_1-i\sigma_2), \tag{57}$$

where σ_1 and σ_2 are real. σ_1 corresponds to the flexibility of the common imperfect interface, whereas σ_2 associated to the viscoelastic parameter of the common imperfect interface. Hence, $\Gamma_1=\Gamma_2=0$ corresponds to the perfect (wielded) interface.

Introducing Γ in the obtained frequency equation Eq. (56), we result in

$$E^0(k)\left[1+\frac{H'\psi^0(k)\Gamma}{4[\mu_T+(\mu_L-\mu_T)a_1^2]k\mu_T}\right]=0. \tag{58}$$

After simplification of Eq.(58), we obtain

$$\tan P_1 H=\frac{\chi_1^0}{\chi_2^0}+i\frac{\chi_3^0}{\chi_2^0}, \tag{59}$$

where $\chi_i^0(i=1,2,3)$ is provided in Appendix B.

The real part of Eq. (59) gives the following dispersion equation for electrically open case

$$\tan kH\sqrt{\frac{c_o^2}{c_1^2}-1}=\frac{\chi_1^0}{\chi_2^0}. \tag{60}$$

with c_o being the phase velocity of Love-type wave for electrically open case.

8. Dispersion equation for electrically short case

Boundary conditions for electrically short case are composed of Eqs. (22)-(26).

Equating the absolute terms (i.e., terms are containing ε) and the coefficient of ε from Eqs. (37), (38), (44), (46) and (47), we obtain the following:

$$\left(\frac{e_{15}}{\varepsilon_{11}}\cos P_1 H\right)A_0^1-\left(\frac{e_{15}}{\varepsilon_{11}}\sin P_1 H\right)B_0^1+C_0^1e^{kH}+D_0^1e^{-kH}=0,$$
$$\left(\frac{e_{15}}{\varepsilon_{11}}\cos P_1 H\right)A_1^1-\left(\frac{e_{15}}{\varepsilon_{11}}\sin P_1 H\right)B_1^1+C_1^1e^{kH}+D_1^1e^{-kH}=0,$$
$$\overline{c_{44}}[A_0^1P_1\sin P_1 H+B_0^1P_1\cos P_1 H]+e_{15}[-C_0^1ke^{kH}+D_0^1e^{-kH}]=0,$$
$$\overline{c_{44}}[A_1^1P_1\sin P_1 H+B_1^1P_1\cos P_1 H]+e_{15}[-C_1^1ke^{kH}+D_1^1e^{-kH}]=0,$$
$$\sigma A_0^1-(\sigma+\xi)E_0^1=\frac{2}{P_2}\sigma e^{-P_2 d}-2\mu_T e^{-P_2 d}+ik(\mu_L-\mu_T)a_1a_2\frac{2}{P_2}e^{-P_2 d},$$
$$A_1^1\sigma+\left[-\sigma-\mu_T P_2-(\mu_L-\mu_T)a_1^2P_2-(\mu_L-\mu_T)ika_1a_2\right]E_1^1=R_1^1(k),$$
$$C_0^1+D_0^1+\frac{e_{15}}{\varepsilon_{11}}A_0^1=0,$$
$$C_1^1+D_1^1+\frac{e_{15}}{\varepsilon_{11}}A_1^1=R_2^1(k),$$

$$-\overline{c_{44}}P_1B_0^1+(ke_{15})C_0^1-(e_{15}k)D_0^1+[-\mu_TP_2-(\mu_L-\mu_T)a_1^2P_2$$
$$-(\mu_L-\mu_T)a_1a_2ik]E_0^1=-2\mu_Te^{-P_2d}-(\mu_L-\mu_T)a_1^2 2e^{-P_2d}$$
$$+ik(\mu_L-\mu_T)a_1a_2\frac{2}{P_2}e^{-P_2d},$$
$$-\overline{c_{44}}P_1B_1^1+(ke_{15})C_1^1-(e_{15}k)D_1^1+[-\mu_TP_2-(\mu_L-\mu_T)a_1^2P_2$$
$$-(\mu_L-\mu_T)a_1a_2ik]E_1^1=R_3^1(k).$$

On solving above equations, we get distinct expressions of A_0^1, B_0^1, C_0^1, D_0^1, E_0^1, A_1^1, B_1^1, C_1^1, D_1^1 and E_1^1 which are provided in Appendix A along with $R_i^1(k)$ for $i=1,2,3$, where the superscript "1" corresponds to the electrically short case.

Therefore, the mechanical displacement in the upper irregular imperfectly bonded piezoelectric layer for electrically short case is given by

$$W_1^1=\frac{1}{2\pi}\int_{-\infty}^{\infty}\frac{X\sin P_1x}{E^1(k)}\left[1+\varepsilon\frac{Y}{X}\right]e^{-iky}dk, \tag{61}$$

where X, Y and $E^1(k)$ are provided in Appendix A.

Now, we calculate

$$Y=\frac{s}{\pi}\int_{-\infty}^{\infty}[\psi^1(k-\lambda)+\psi^1(k+\lambda)]\frac{1}{\lambda}\sin\left(\frac{\lambda s}{2}\right)d\lambda, \tag{62}$$

where $\psi^1(k-\lambda)=[B_2+B_3+B_4]^{\eta=k-\lambda}$,

and B_2, B_3 and B_4 are defined in appendix A.

Using asymptotic formula of willis (1948) and Tranter (1966), we result in

$$\int_{-\infty}^{\infty}[\psi^1(k-\lambda)+\psi^1(k+\lambda)]\frac{1}{\pi}\sin(\frac{\lambda s}{2})d\lambda\cong\frac{\pi}{2}2\psi^1(k)=\pi\psi^1(k). \tag{63}$$

Now, using Eq. (63) in Eq. (62), we obtain

$$Y=\frac{s}{\pi}\pi\psi^1(k)=s\psi^1(k)=\frac{H'}{\varepsilon}\psi^1(k). \tag{64}$$

With the help of Eq. (64), Eq. (61) gives the required mechanical displacement of the irregular imperfectly bonded piezoelectric layer as

$$W_1^1=\frac{1}{2\pi}\int_{-\infty}^{\infty}\frac{X\sin P_1x}{E^1(k)\left[1-\frac{H'\psi^1(k)}{X}\right]}e^{-iky}dk. \tag{65}$$

The value of this integral depends upon the contribution of poles of the integrand. In order to find the pole, we calculate the roots of the following equation

$$E^1(k)\left[1-\frac{H'\psi^1(k)}{X}\right]=0. \tag{66}$$

Eq. (66) may further be expressed as in the form

$$E^1(k)\left[1-\frac{H'\psi^1(k)\Gamma}{X}\right]=0. \tag{67}$$

After simplification of Eq. (66), we obtain

$$\tan P_1H=\frac{\chi_1^1}{\chi_2^1}+i\frac{\chi_3^1}{\chi_2^1}, \tag{68}$$

where $\chi_i^1(i=1,2,3)$ is provided in Appendix B.

The real part of Eq. (68) gives the following dispersion equation for electrically short case

$$\tan kH\sqrt{\frac{c_s^2}{c_1^2}-1}=\frac{\chi_1^1}{\chi_2^1}. \tag{69}$$

with c_s being the phase velocity of Love-type wave for electrically short case.

9. Particular cases and validation

In this section, discussion is made for four particular cases of the considered problem.

9.1 Case-I

When the composite structure consists of imperfectly bonded piezoelectric layer with a lower fiber-reinforced half-space having no irregularity at the common interface (i.e., H'=0), the dispersion equations for electrically open and short case respectively takes the following form.

9.1.1 For electrically open case

The dispersion relation (60) in absence of an irregularity at the common interface reduces to

$$\tan\sqrt{\left(\frac{c_o^2}{c_1^2}-1\right)}kH=\frac{G_1^0G_2^0+G_3^0G_4^0}{(G_1^0)^2+(G_3^0)^2}, \tag{70}$$

where $G_i^0(i=1,2,3)$ is provided in Appendix B.

9.1.2 For electrically short case

Dispersion relation (69) for electrically short case in absence of an irregularity at the common interface reduces to

$$\tan\sqrt{\left(\frac{c_s^2}{c_1^2}-1\right)}kH=\frac{G_1^1G_2^1+G_3^1G_4^1}{(G_1^1)^2+(G_3^1)^2}, \tag{71}$$

where $G_i^1(i=1,2,3)$ is provided in Appendix B.

9.2 Case-II

When the composite structure constituted by perfectly bonded (i.e., $\Gamma=\Gamma_1-i\Gamma_2=0$) piezoelectric layer with lower fiber-reinforced half-space having an rectangular shaped irregularity at the common interface, the dispersion equation for electrically open and short case transforms in the following way

9.2.1 For electrically open case

In electrically open case with perfect bonding between the layer and the half-space, the dispersion relation Eq. (60) transform to

$$\tan\sqrt{\left(\frac{c_o^2}{c_1^2}-1\right)}kH=\frac{\chi_4^0}{\chi_5^0}, \tag{72}$$

where $\chi_i^0\,(i=4,5)$ is provided in Appendix C.

9.2.2 For electrically short case

In electrically open case with perfect bonding between the layer and the half-space, the dispersion relation Eq.(69) transform to

$$\tan\sqrt{\left(\frac{c_s^2}{c_1^2}-1\right)}kH=\frac{\chi_4^1}{\chi_5^1}, \tag{73}$$

where $\chi_i^1\,(i=4,5)$ is provided in Appendix C.

9.3 Case-III

When the composite structure is comprised of an isotropic layer (i.e., e_{15}=0) perfectly bonded (i.e., Γ=0) with an isotropic half-space (i.e., $\mu_T=\mu_L=\tilde{\mu}_0$) and having a rectangular shaped irregularity at the common interface, the obtained dispersion relations for open and short case i.e., Eqs. (60) and (69) may be obtained as follows

$$\tan P_1^*H=\frac{\mu_0\tilde{\mu}_0P_1^*s_2^*+H'[\tilde{\mu}_0^2k(s_2^*)^2-\mu_0^2(P_1^*)^3]-(H')^2[\mu_0\tilde{\mu}_0ks_2^*(P_1^*)^2]}{\mu_0^2(P_1^*)^2+2H'\mu_0P_1^*k\tilde{\mu}_0s_2^*+(H')^2(k\tilde{\mu}_0s_2^*)^2}, \tag{74}$$

where $c_o=c_s=c^*$ and $P_1^*=k\sqrt{(\frac{(c^*)^2}{\beta_0^2}-1}$, $s_2^*=k\sqrt{1-\frac{(c^*)^2}{\tilde{\beta}_0^2}}$; $\beta_0=\sqrt{\frac{\mu_0}{\rho_0}}$ and $\tilde{\beta}_0=\sqrt{\frac{\tilde{\mu}_0}{\tilde{\rho}_0}}$; μ_0 and $\tilde{\mu}_0$ being Lamé paramaters and ρ_0 and $\tilde{\rho}_0$ are the material density of the isotropic layer and isotropic elastic half-space respectively.

9.4 Case-IV

When the isotropic layer (i.e., e_{15}=0) is perfectly bonded (i.e., Γ=0) with isotropic elastic half-space (i.e., $\mu_L=\mu_T=\tilde{\mu}_0$) in a composite structure without having any irregularity (i.e., *H′*=0) at the common interface, the real part of the obtained dispersion relations for open and short case i.e., Eqs. (60) and (69) is found in well-agreement to the following Classical Love wave equation

$$\tan P_1^*H=\frac{\tilde{\mu}_0s_2^*}{\mu_0P_1^*}. \tag{75}$$

10. Numerical calculation and discussion

In order to illustrate the theoretical results for the deduced closed-form of dispersion equation for the propagation of Love-type wave in a composite structure comprised of an imperfectly bonded piezoelectric layer lying over a fiber-reinforced half-space with rectangular irregularity at the common interface Figs. 2-8 have been plotted. In these figures, variation of non-dimensional phase velocity against non-dimensional wave number has been studied to reveal the influence of various affecting parameters on dispersion curve in reinforced and reinforced-free composite structure for both electrically open and short cases. Through referential figures, the influence of reinforcement in composite structure, irregularity parameter (*H′*/*H*) associated with irregularity at the common interface, flexibility imperfectness parameter (Γ_1) and viscoelastic imperfectness parameter (Γ_2) associated with the complex common interface, piezoelectric coefficient (e_{15}) and dielectric constant (e_{11}) has been shown. For the purpose of numerical computations, we consider the following data:

(i) For the upper imperfectly bonded irregular piezoelectric layer (Tiersten 1969):

$e_{15}=2.6\,C/m^2,\ \varepsilon_{11}=3.63\times10^{-10}\,C/Nm^2,$

$c_{44}=9.4\times10^{10}\,N/m^2,\ \rho_1=7450\,Kg/m^3.$

(ii) For the lower fiber-reinforced half-space (Gilis 1984) (Pierson 2012):

$\mu_L=0.23\times10^{10}\,N/m^2,\ \mu_T=44.5\times10^{10}\,N/m^2,$

$\rho_2=2260\,Kg/m^3.$

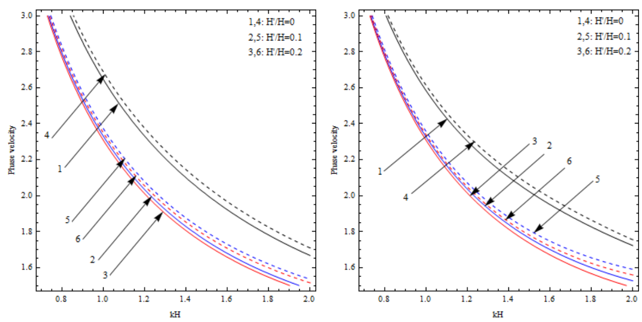

(a) (b)

Fig. 2 The variation of non-dimensional phase velocity against non-dimensional wave number for different values of irregularity parameter (*H′*/*H*) in composite structure (a) with reinforcement and (b) without reinforcement for both electrically open and short case

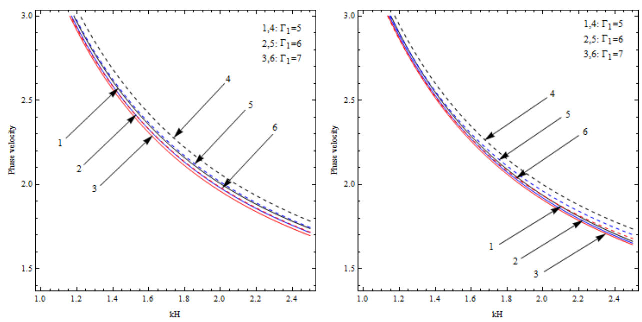

(a) (b)

Fig. 3 The variation of non-dimensional phase velocity against non-dimensional wave number for different values of flexibility imperfectness parameter (Γ_1) at complex common irregular interface of the composite structure (a) with reinforcement and (b) without reinforcement for both electrically open and short case

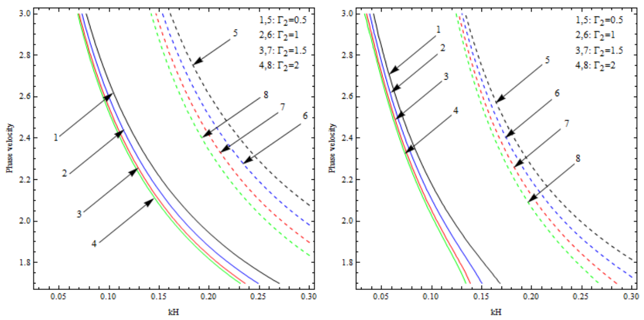

(a) (b)

Fig. 4 The variation of non-dimensional phase velocity against non-dimensional wave number for different values of viscoelastic imperfectness parameter (Γ_2) at complex common irregular interface of the composite structure (a) with reinforcement and (b) without reinforcement for both electrically open and short case

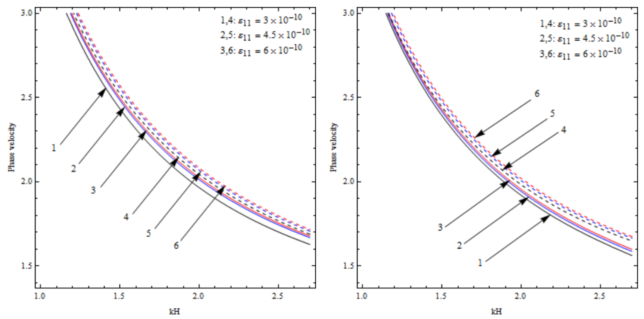

(a) (b)

Fig. 5 The variation of non-dimensional phase velocity against non-dimensional wave number for different values of dielectric constant (ε_{11}) in composite structure (a) with reinforcement and (b) without reinforcement for both electrically open and short case

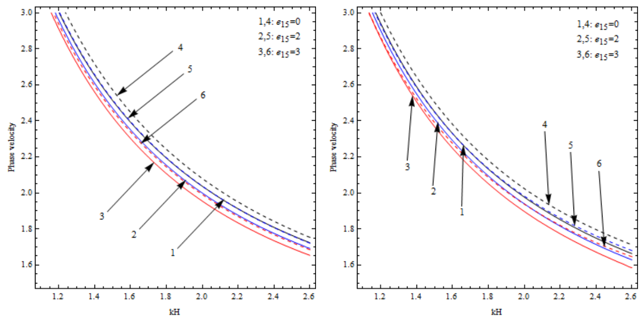

(a) (b)

Fig. 6 The variation of non-dimensional phase velocity against non-dimensional wave number for different values of piezoelectric coefficient (e_{15}) in composite structure (a) with reinforcement and (b) without reinforcement for both electrically open and short case

Moreover, we consider (Hool and Kinne 1924): $a_1 = 0.00316227$

In these figures, it is revealed that phase velocity of Love-type wave decreases with the increase in wave number in reinforced and reinforced-free composite structure for both electrically open and short cases

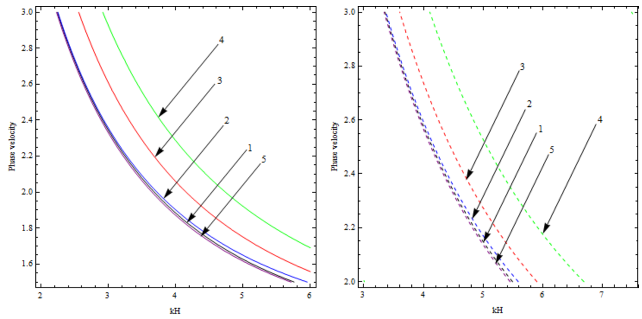

(a) (b)

Fig. 7 The variation of non-dimensional phase velocity against non-dimensional wave number in distinct cases associated with irregularity and imperfectness in reinforced and reinforced-free composite structure for (a) electrically open case, and (b) electrically short case

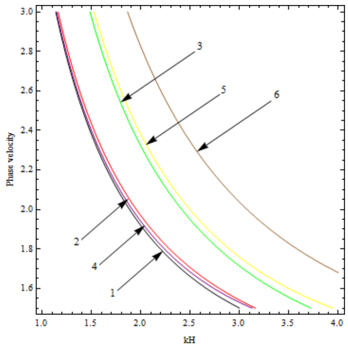

Fig. 8 The variation of non-dimensional phase velocity against non-dimensional wave number in distinct cases associated with presence and absence of piezoelectricity in reinforced and reinforced-free composite structure with imperfect and perfect common interface for electrically open and short case

irrespective of presence or absence of irregularity, imperfectness of common interface and piezoelectricity associated with layer. Solid line curves in all the figures correspond to electrically open case whereas dashed line curves correspond to electrically short case. Figs. 2(a), 3(a), 4(a), 5(a) and 6(a) are associated with the case when Love-type wave is propagating in a reinforced composite structure for both electrically open and short cases whereas Figs. 2(b), 3(b), 4(b), 5(b) and 6(b) are associated with the case when Love-type wave is propagating in a reinforced-free composite structure for both electrically open and short cases.

In Figs. 2(a) and 2(b), the effect of irregularity parameter (H'/H) associated with the rectangular irregularity at the common interface on phase velocity of Love-type wave propagating in reinforced and reinforced-free composite structure has been shown for both electrically open and short cases. In these figures, curves 1 and 4 depict the case when the composite structure doesn't contains irregularity at the common interface of layer and half-space whereas curves 2, 3, 5 and 6 manifest the case of composite structure containing irregularity. More specifically, curves 1 and 4 in Fig. 2(a) correspond to Case-I whereas curves 1 and 4 in Fig. 2(b) correspond to Case-I but without reinforcement. It is revealed from these figures that phase velocity of Love-type wave decreases with the increase of depth of irregularity for both electrically open and short cases irrespective of the situation that composite structure is reinforced or reinforced-free.

The influence of flexibility imperfectness parameter (Γ_1) associated with the complex common irregular interface on phase velocity of Love-type wave propagating in the composite structure with reinforcement and without reinforcement has been shown in Figs. 3(a) and 3(b) respectively each with electrically open and short cases. These figures reveal that the phase velocity of Love-type wave propagating in the composite structure decreases with the increase in flexibility imperfectness parameter for both electrically open and short cases irrespective of the presence or absence of reinforcement in the composite structure.

In Figs. 4(a) and 4(b) the effect of viscoelastic imperfectness parameter (Γ_2) associated with the complex common irregular interface on phase velocity of Love-type wave propagating in the reinforced and reinforced-free composite structure has been displayed respectively each with electrically open and short cases. These figures illustrate that the phase velocity of Love-type wave decreases with the increase in viscoelastic imperfectness parameter for both electrically open and short cases irrespective of the situation that composite structure is reinforced or reinforced-free.

The figures 3(a), 3(b), 4(a) and 4(b) depict that imperfectness of the common irregular interface between the layer and half-space of reinforced and reinforced-free composite structure disfavours the phase velocity of Love-type wave for both electrically open and short cases.

The effect of dielectric constant (ε_{11}) associated with piezoelectric layer in composite structure on phase velocity of Love-type wave has been demonstrated in Figs. 5(a) and 5(b) for the case of composite structure with reinforcement and without reinforcement respectively in both electrically open and short conditions. These figures portray that the phase velocity of Love-type wave increases with the increase in dielectric constant for both electrically open and short cases in reinforced or reinforced-free composite structure.

In Figs. 6(a) and 6(b), the influence of piezoelectric coefficient (ε_{11})associated with piezoelectric layer in composite structure on phase velocity of Love-type wave has been elucidated for the composite structure with reinforcement and without reinforcement respectively each with electrically open and short cases. In Fig. 6(a), curves 1 and 4 manifest the case when the Love-type wave is propagating in the composite structure comprised of imperfectly bonded isotropic layer with lower fiber-reinforced half-space with irregular common interface whereas as curves 1 and 4 in Fig. 6(b) depict the case of propagation of Love-type wave through the composite structure comprised of imperfectly bonded isotropic layer with lower isotropic elastic half-space with irregular common interface. These figures portray that the phase velocity of Love-type wave decreases with the increase in piezoelectric coefficient for both electrically open and short conditions irrespective of the presence and absence of reinforcement in the composite structure. It can be concluded from the figures 5(a), 5(b), 6(a) and 6(b) that piezoelectricity associated with layer disfavours the phase velocity of Love-type wave propagating in both reinforced and reinforced-free composite structure. Meticulous examination of Figs. 2(a) to 6(b) in a comparative approach, it can be traced out that reinforcement in the composite structure favours the phase velocity of Love-type wave.

To unravel the effect of irregularity, imperfectness associated with the common interface and reinforcement of the composite structure on phase velocity of Love-type wave, Figs. 7(a) and 7(b) have been illustrated. Curve 1 in Figs. 7(a) and 7(b) represents the phase velocity of Love-type wave propagating in composite structure comprised of imperfectly bonded piezoelectric layer with lower fiber-reinforced half-space with rectangular shaped irregularity at the common interface for electrically open and short case respectively whereas curve 2 illustrates the case when the considered composite structure is having no irregularity at the common interface (i.e., Case-I) for electrically open and short case respectively. Curve 3 in Figs. 7(a) and 7(b) manifests the dispersion of Love-type wave propagating in the composite structure comprised of perfectly bonded piezoelectric layer with lower fiber-reinforced half-space with rectangular shaped irregularity at the common interface (i.e., Case-II) for the open and short case respectively whereas curve 4 in Figs. 7(a) and 7(b) portrays the case when the composite structure is having no irregularity and contains perfectly bonded common interface for electrically open and short case respectively. Curve 5 shows the case when the considered composite structure is reinforced-free for electrically open and short case. The comparative study of these curves in both the figures reveals that imperfectness at the common interface disfavours phase velocity of Love-type wave more as compared to the irregularity at the common interface in the composite structure in both electrically open and short conditions. It has been found that the phase velocity of Love-type wave is more in absence of imperfectness and irregularity at the common interface of the composite structure for both electrically open and short cases. It has also been reported that the phase velocity is least in absence of reinforcement in the composite structure for electrically open and short conditions irrespective of the absence or presence of irregularity and imperfectness at the common interface of the composite structure.

The comparative study between the particular cases (Case I, II, III and IV) has been demonstrated in Fig. 8. Curve 1 in this figure illustrates the dispersion of Love-type wave propagating in composite structure comprised of imperfectly bonded piezoelectric layer lying over a fiber-reinforced half-space with rectangular shaped irregularity at the common interface whereas curve 2 represents the case of absence of piezoelectricity in the composite structure. In Fig. 8, curve 3 shows the dispersion of Love-type wave propagating in the composite structure comprised of perfectly bonded isotropic layer with lower fiber-reinforced half-space with rectangular irregularity at the common interface whereas curve 4 portrays the case when the composite structure is comprised of imperfectly bonded isotropic layer with lower isotropic elastic half-space with rectangular irregular common interface. In this figure, curve 5 demonstrates the case when the composite structure is comprised of perfectly bonded isotropic layer with lower isotropic elastic half-space with irregular common interface (Case-III) whereas Curve 7 represents the case when the composite structure is comprised of perfectly bonded isotropic layer and half-space without irregularity at the common interface (Case-IV) which is the model for the Classical Love wave equation. The curves in this figure reveal that when the composite structure is considered to be free from piezoelectricity, imperfectness associated with the irregular common interface disfavours the phase velocity of Love-type wave irrespective of the presence or absence of reinforcement in the composite structure. The effect of imperfectness associated with the irregular common interface on phase velocity of Love-type wave is found to be more in case of composite structure without piezoelectricity and reinforcement as compared to the case when the composite structure is only without piezoelectricity. It has also been also reported that the phase velocity increase more when the composite structure is comprised of isotropic layer and half-space without irregularity and imperfectness at the common interface (i.e., Case-IV). The comparative study of the particular cases reveals that the phase velocity of Love type wave in the composite structure is more in Case-III as compared to the Case-II. The study also reveals that the phase velocity of Love type wave in the composite structure is maximum for Case-IV whereas it is found to be minimum for Case-I.

10. Conclusions

The present study articulates the propagation of Love-type wave in a composite structure comprised of an imperfectly bonded piezoelectric layer and a lower fiber-reinforced half-space with rectangular shaped irregularity at the common interface. Dispersion relation has been deduced analytically in closed-form for electrically open and short conditions and further as a special case it is found in well-agreement to the classical Love-wave equation. It has been established through the study that wave-length, reinforcement in the composite structure, irregularity parameter (H'/H), flexibility imperfectness parameter (Γ_1) and viscoelastic imperfectness parameter (Γ_2) associated with the complex common interface, piezoelectric coefficient (e_{15}) and dielectric constant (ε_{11}) have significant effects on the phase velocity in the composite structure in all the studied cases. Numerical computation and graphical demonstration have been carried out to show the effects of these parameters on the phase velocity of Love-type wave in the composite structure in all the distinct cases. The outcome of the present study can be encapsulated as follows:

(i) The phase velocity of Love-type wave decrease with the increase in wave number in the composite structure in all the studied cases.

(ii) Phase velocity of Love-type wave for both electrically open and short cases decreases with the increase in irregularity parameter irrespective of the presence or absence of imperfectness associated with the common interface, piezoelectricity and reinforcement in the composite structure.

(iii) The presence of imperfectness at the irregular common interface decrease the phase velocity of Love-type wave irrespective of the presence or absence of irregularity associated with the common interface, piezoelectricity and reinforcement in the composite structure in both electrically open and short cases.

(iv) The phase velocity of Love-type wave decrease with the increase in piezoelectric coefficient whereas the presence of dielectric constant increase the phase velocity of Love-type wave in the reinforced and reinforced-free composite structure in all the studied cases. In a way, piezoelectricity disfavours phase velocity of Love-type wave in the considered reinforced and reinforced-free composite structure in all the distinct cases.

(v) Phase velocity of Love-type wave for the electrically short case is found to be more as compared to the electrically open case for the reinforced and reinforced-free composite structure in all the studied cases.

(vi) Phase velocity of Love-type wave is found to be more for the reinforced composite structure as compared to the case when composite structure is without reinforcement. In a conclusive way, reinforcement in composite structure favours phase velocity of Love-type wave.

(vii) The effect of irregularity and imperfectness associated with the common interface of the composite structure on phase velocity of Love-type wave is found to be more when the composite structure is without piezoelectricity as compared to the case when the composite structure is without reinforcement.

The present study may have its possible applications in the sphere of civil engineering, earth science engineering and seismology.

The consequences of the theoretical study in the framework of the considered model can be employed in the field of acoustics, civil engineering, earth science engineering and seismology. The results of the above study may also find its possible application in several devices like acoustic devices, Love wave sensor, transducers, actuators or any other sensor devices to enhance the performance. Acoustic emissions in a stressed structure are detected by an array of highly sensitive piezoelectric transducers that measure the surface displacements caused by stress waves originated from defect sites. It is well-known that signal attenuation in fiber-reinforced polymers is high. Low frequency waves (typically 20-111 kHz) attenuate less and therefore they travel longer distances than high-frequency waves. As a result transducers prefer fiber-reinforced composite structures along with piezoelectric composites. In Love wave sensor, in particular, mass density, elastic stiffness, and dielectric properties increase the sensing response. Any change in these properties leads to the changes in phase velocity of the acoustic wave. The outcome of the present study unlocks the possibility of the implementation of piezoelectric layer (guiding layer) mounted on a fiber-reinforced semi-infinite medium in Love wave sensor or in any new type of devices for the propagation of Love-type wave. It is reported from the above study that the presence of reinforcement in the medium increase the phase velocity of Love-type wave and hence it is favourable for the confinement of the wave propagating at the interface of the guiding layer and reinforced half-space. Sensitivity increase with the increase in confinement of the wave in the guiding layer. Thus, the presence of irregularity and its effect on phase velocity of Love-type wave considered in the present study. The irregularity appreciate the delay of the confinement of the wave for a longer period in the guiding layer. The mounting may not be perfectly welded. The above study also discussed the influence of imperfectness parameter in the present model which is close to the real life scenario. Thus the results achieved in the present study may be considered for the proper design of these devices.

Acknowledgements

The authors convey their sincere thanks to Indian Institute of Technology (Indian School of Mines), Dhanbad for providing JRF to Mr. Mriganka Shekhar Chaki and also facilitating us with its best facility for research. The authors also convey their sincere thanks to Department of Science and Technology, Science & Engineering Research Board (DST-SERB) for their financial support to carry out this research work through Project no. EMR/2016/003985/MS entitled "Mathematical Study on Wave Propagation Aspects in Piezoelectric Composite Structures with Complexities ".

References

Auld, B.A. (1990), *Acoustic Fields and Waves in Solids*, 1&2, Krieger, Malabar, FL.

Belfield, A.J., Rogers, T.G. and Spencer, A.J.M. (1983), "Stress in elastic plates reinforced by fibers lying in concentric circles", *J. Mech. Phys. Solid.*, **31**(1), 25-54

Bhattacharya, J. (1962), "On the dispersion curve for Love wave due to irregularity in the thickness of the transversely isotropic crustal layer", *Gerlands Beitrage zur Geophysik*, **6**, 324-334.

Chattopadhyay, A. and Singh, A.K. (2012), "Propagation of magnetoelastic shear waves in an irregular self-reinforced layer", *J. Eng. Math.*, **75**, 139-155.

Chattopadhyay, A., Gupta, S., Sahu, S.A. and Singh, A.K. (2012), "Dispersion of horizontally polarized shear waves in an irregular non-homogeneous self reinforced crustal layer over a semi-infinite self- reinforced medium", *J. Vib. Control*, **19**, 109-119.

Chattopadhyay, A., Gupta, S., Sharma, V.K. and Kumari, P. (2008), "Propagation of SH waves in an irregular monoclinic crustal layer", *Arch. Appl. Mech.*, **78**(12), 989-999.

Chen, W.Q. and Lee, K.Y. (2004), "Exact solution of angle-ply piezoelectric laminates in cylindrical bending with interfacial imperfections", *Compos. Struct.*, **65**(3), 329-337.

Curie, J. and Curie, P. (1880), "Development by pressure of polar

Du, J., Jin, X., Wang, J. and Xian, K. (2007), "Love wave propagation in functionally graded piezoelectric material layer", *Ultrasonics*, **46**, 13-22.

Du, J., Xian, K., Wang, J. and Yong, Y.K. (2008), "Propagation of Love waves in prestressed piezoelectric layered structures loaded with viscous liquid", *Acta Mech Solida Sin*, **21**, 542-548.

electricity in hemihedral crystals with inclined faces", *Bull. Soc. Min. de France*, **3**, 90.

Eskandari, M. and Shodja, H.M. (2008), "Love waves propagation in functionally graded piezoelectric materials with quadratic variation", *J. Sound Vib.*, **313**, 195-204.

Gillis, P.P. (1984), "Calculating the elastic constants of graphite", *Carbon*, **22**(4), 387-391.

Hashin, Z. and Rosen, W.B. (1964), "The elastic moduli of fibre reinforced materials", *J. Appl. Mech.*, **31**, 223- 232.

Hool, G.A. and Kinne, W.S. (1924), *Reinforced Concrete and Masonry Structure*, McGrawHill, New York

Jakoby, B. and Vellekoop, M.J. (1997), "Properties of Love waves: applications in sensors", *Smart Mater. Struct.*, **6**, 668-679.

Kaur, T., Sharma, S.K. and Singh, A.K. (2016), "Influence of imperfectly bonded micropolar elastic half-space with non-homogeneous viscoelastic layer on propagation behavior of shear wave", *Waves Random Complex*, **26**(4), 650-670.

Kaur, T., Singh, A.K., Chattopadhyay, A. and Sharma, S.K. (2014), "Dynamic response of normal moving load on an irregular fiber-reinforced half-space", *J. Vib. Control*, **22**(1), 77-88.

Li, P. and Jin, F. (2015), "Excitation and propagation of shear horizontal waves in a piezoelectric layer imperfectly bonded to a metal or elastic substrate", *Acta Mech.*, **226**(2), 267-284.

Li, X.Y., Wang, Z.K. and Huang, S.H. (2004), "Love waves in functionally graded piezoelectric materials", *Int. J. Solid. Struct.*, **41**, 7309-7328.

Liu, H., Wang, Z.K. and Wang, T.J. (2001), "Effect of initial stress on the propagation behavior of Love waves in a layered piezoelectric structure", *Int. J. Solid. Struct.*, **38**, 37-51.

Liu, J. and He, S. (2010), "Properties of Love waves in layered piezoelectric structures", *Int. J. Solid. Struct.*, **47**, 169-174.

Liu, J.X., Fang, D.N., Wei, W.Y. and Zhao, X.F. (2008), "Love waves in layered piezoelectric/piezomagnetic structures", *J. Sound Vib.*, **315**, 146-156.

Nagy, P.B. (1992), "Ultrasonic classification of imperfect interfaces", *J. Nondestruct. Eval.*. **11**, 127-139.

Otero, J.A., Rodríguez-Ramos, R., Bravo-Castillero, J. and Monsivais, G. (2012), "Interfacial waves between two piezoelectric half-spaces with electro-mechanical imperfect interface", *Philos. Mag.*, **92**(10), 534-540.

Pang, Y., Wang, Y.S., Liu, J.X. and Fang, D.N. (2008), "Reflection and refraction of plane waves at the interface between piezoelectric and piezomagnetic media", *Int. J. Eng. Sci.*, **46**, 1098-1110.

Pierson, H.O. (2012), *Handbook of Carbon, Graphite, Diamonds and Fullerenes: Processing, Properties and Applications*, William Andrew.

Piliposian, G.T. and Danoyan, Z.N. (2009), "Surface electro-elastic Love waves in a layered structure with a piezoelectric substrate and two isotropic layers", *Int. J. Solid. Struct.*, **46**, 1345-1353.

Qian, Z., Jin, F., Wang, Z. and Kishimoto, K. (2007), "Transverse surface waves on a piezoelectric material carrying a functionally graded layer of finite thickness", *Int. J. Eng. Sci.*, **45**, 455-466.

Schoenberg, M. (1980), "Elastic wave behavior across linear slip interfaces", *J. Acoust. Soc. Am.*, **68**, 1516-1521.

Singh, A.K., Kumar, S. and Chattopadhyay, A. (2015), "Love-type wave propagation in a piezoelectric structure with irregularity", *Int. J. Eng. Sci.*, **89**, 35-60.

Singh, B. (2006), "Wave propagation in thermally conducting linear fibre-reinforced composite materials", *Arch. Appl. Mech.*, **75**(8-9), 513-520.

Termonia, Y. (1990), "Fibre coating as a means to compensate for

poor adhesion in fibre-reinforced materials", *J. Mater. Sci.*, **25**, 103-106.
Tiersten, H.F. (1969), *Linear Piezo-electric Plate Vibration*, Plenum Press, New York.
Tiersten, H.F. (1969), *Linear Piezoelectric Plate Vibrations*, Plenum Press, New York, NY.
Tranter, C.J. (1966), *Integral Transforms in Mathematical Physics*, Methuen and Co. Ltd., London.
Willis, H.F. (1948), "A formula for expanding an integral as a series", *Philosoph. Mag.*, **39**, 455-459.

CC

Appendix A

$$\xi = \mu_T P_2 + (\mu_L - \mu_T) a_1^2 P_2 + (\mu_L - \mu_T) a_1 a_2 ik,$$

$$E^0(k) = \overline{c_{44}} \tan P_1 H \varepsilon_{11} (1 + e^{2kH})(\sigma + \xi) P_1 - k e_{15}^2 (1 - e^{2kH})(\sigma + \xi) - \sigma \xi \varepsilon_{11} (1 + e^{2kH}),$$

$$\xi_1 = \mu_T P_2 + (\mu_L - \mu_T) a_1^2 P_2 - (\mu_L - \mu_T) a_1 a_2 ik,$$

$$E^1(k) = \alpha_1 \beta_2 - \alpha_2 \beta_1,$$

where

$$\alpha_1 = \bar{c}_{44} P_1 \tan P_1 H - \frac{e_{15}^2}{\varepsilon_{11}} k \left(\frac{e^{kH}}{e^{kH} - e^{-kH}} \right) \sec P_1 H + \frac{e_{15}^2}{\varepsilon_{11}} k \left(\frac{e^{kH} + e^{-kH}}{e^{kH} - e^{-kH}} \right),$$

$$\beta_1 = \bar{c}_{44} P_1 - \frac{e_{15}^2}{\varepsilon_{11}} k \left(\frac{e^{kH} + e^{-kH}}{e^{kH} - e^{-kH}} \right) \tan P_1 H,$$

$$\alpha_2 = \frac{e_{15}^2 k}{\varepsilon_{11} \sec P_1 H} \frac{[(e^{kH} + e^{-kH}) \sec P_1 H - 2]}{(e^{kH} - e^{-kH})} - \frac{\sigma \xi}{\sigma + \xi},$$

$$\beta_2 = -\bar{c}_{44} P_1 + \frac{2 e_{15}^2}{\varepsilon_{11}} \frac{\tan P_1 H}{\sec P_1 H (e^{kH} + e^{-kH})}.$$

$$A_0^0 = -\frac{4 e^{-P_2 d} \sigma \varepsilon_{11} (1 + e^{2kH})(\mu_T + (\mu_L - \mu_T) a_1^2)}{E^0(k)},$$

$$B_0^0 = \frac{4 e^{-P_2 d} \sigma \varepsilon_{11} (1 + e^{2kH})(\mu_T + (\mu_L - \mu_T) a_1^2) \tan P_1 H}{E^0(k)},$$

$$C_0^0 = \frac{4 e^{-P_2 d} \sigma (\mu_T + (\mu_L - \mu_T) a_1^2) e_{15}}{E^0(k)},$$

$$D_0^0 = \frac{4 e^{-P_2 d} \sigma e^{2kH} (\mu_T + (\mu_L - \mu_T) a_1^2) e_{15}}{E^0(k)},$$

$$E_0^0 = -\frac{\begin{aligned} & 4 e^{-P_2 d} \sigma^2 \varepsilon_{11} (1 + e^{2kH})(\mu_T + (\mu_L - \mu_T) a_1^2) \\ & + E^0(k) \left[\frac{2}{P_2} \sigma e^{-P_2 d} + 2 \mu_T e^{-P_2 d} + (\mu_L - \mu_T) a_1 \times \left(2 e^{-P_2 d} a_1 - ik a_2 \frac{2}{P_2} e^{-P_2 d} \right) \right] \end{aligned}}{E^0(k)(\sigma + \xi)},$$

$$A_1^0 = \frac{\varepsilon_{11} (1 + e^{2kH}) \left[R_3^0(k)(\sigma + \xi) - \left(\frac{1 - e^{2kH}}{1 + e^{2kH}} \right) k e_{15} \times R_2^0(k)(\sigma + \xi) - R_1^0(k) \xi \right]}{E^0(k)},$$

$$B_1^0 = -\frac{\varepsilon_{11} (1 + e^{2kH}) \left[R_3^0(k)(\sigma + \xi) - \left(\frac{1 - e^{2kH}}{1 + e^{2kH}} \right) k e_{15} \times R_2^0(k)(\sigma + \xi) - R_1^0(k) \xi \right] \tan P_1 H}{E^0(k)},$$

$$C_1^0 = \frac{R_2^0(k) E^0(k) - e_{15} (1 + e^{2kH}) \left[R_3^0(k)(\sigma + \xi) - \left(\frac{1 - e^{2kH}}{1 + e^{2kH}} \right) k e_{15} \times R_2^0(k)(\sigma + \xi) - R_1^0(k) \xi \right]}{E^0(k)(1 + e^{2kH})},$$

$$D_1^0=\frac{R_2^0(k)}{1+e^{2kH}}-\frac{e_{15}(1+e^{2kH})R_3^0(k)(\sigma+\xi)-(\frac{1-e^{2kH}}{1+e^{2kH}})ke_{15}\times R_2^0(k)(\sigma+\xi)-R_1^0(k)\xi}{E^0(k)},$$

$$E_1^0=\frac{\varepsilon_{11}(1+e^{2kH}\sigma)R_3^0(k)(\sigma+\xi)-(\frac{1-e^{2kH}}{1+e^{2kH}})ke_{15}R_2^0(k)(\sigma+\xi)-R_1^0(k)\xi-R_1^0(k)E^0(k)}{(\sigma+\xi)E^0(K)},$$

$$\begin{aligned}R_1^j(k)=\frac{\varepsilon}{2\pi}\int_{-\infty}^{\infty}\Big[&-P_2E_0^j\sigma+2e^{-P_2d}\sigma-B_0^jP_1\sigma-\mu_TE_0^jP_2^2\\&-2P_2\mu_Te^{-P_2d}-(\mu_L-\mu_T)a_1\big[a_1E_0^jP_2^2+2a_1e^{-P_2d}P_2\\&+ika_2E_0^jP_2-2ika_2e^{-P_2d}\big]+i\lambda\Big\{\Big(\mu_TE_0^j+\frac{2}{P_2}\mu_Te^{-P_2d}\Big)\\&\times(-ik)+(\mu_L-\mu_T)a_2\big[a_1(-P_2E_0^j+2e^{-P_2d})\\&-ika_2\Big(E_0^j+\frac{2}{P_2}e^{-P_2d}\Big)\big]\Big\}\Big]^{\eta=k-\lambda}\bar{h}(\lambda)d\lambda,\end{aligned}$$

(for $j=0,1$)

$$R_2^j(k)=\frac{\varepsilon}{2\pi}\int_{-\infty}^{\infty}\left[C_0^jk-D_0^jk-\frac{e_{15}}{\varepsilon_{11}}(B_0^jP_1)\right]^{\eta=k-\lambda}\bar{h}(\lambda)d\lambda,$$

$$\begin{aligned}R_3^j(k)=\frac{\varepsilon}{2\pi}\int_{-\infty}^{\infty}\Big[&-c_{44}A_0^jP_1^2+e_{15}\left(k^2C_0^j+D_0^jk^2+\frac{e_{15}}{\varepsilon_{11}}(-A_0^jP_1^2)\right)\\&-\mu_TP_2^2E_0^j-\mu_T2e^{-P_2d}P_2-(\mu_L-\mu_T)a_1\big[a_1(P_2^2E_0^j+2e^{-P_2d}P_2)\\&-ika_2(-P_2E_0^j+2e^{-P_2d})\big]+i\lambda\Big\{(c_{44}A_0^j)(-ik)+e_{15}[C_0^j+D_0^j\\&+\frac{e_{15}}{\varepsilon_{11}}A_0^j(-ik)]-\Big\{(-i\eta)(\mu_TE_0^j+\frac{2}{P_2}\mu_Te^{-P_2d})+(\mu_L-\mu_T)a_2\\&\times[a_1(-P_2E_0^j+2e^{-P_2})-i\eta a_2(E_0^j+\frac{2}{P_2}e^{-P_2d})]\Big\}\Big\}\Big]^{\eta=k-\lambda}\bar{h}(\lambda)d\lambda,\end{aligned}$$

$$\begin{aligned}A_2=(\sigma+\xi)\Big[&-c_{44}A_0^0P_1^2+e_{15}\left(k^2C_0^0+D_0^0k^2+\frac{e_{15}}{\varepsilon_{11}}(-A_0^0P_1^2)\right)\\&-\mu_TP_2^2E_0^0-\mu_T2e^{-P_2d}P_2-(\mu_L-\mu_T)a_1\big[a_1(P_2^2E_0^0+2e^{-P_2d}P_2)\\&-ika_2(-P_2E_0^0+2e^{-P_2d})\big]+i\lambda\Big\{(c_{44}A_0^0)(-ik)+e_{15}[C_0^0+D_0^0\\&+\frac{e_{15}}{\varepsilon_{11}}A_0^0(-ik)]-\Big\{(-i\eta)(\mu_TE_0^0+\frac{2}{P_2}\mu_Te^{-P_2d})+(\mu_L-\mu_T)a_2\\&\times[a_1(-P_2E_0^0+2e^{-P_2})-i\eta a_2(E_0^0+\frac{2}{P_2}e^{-P_2d})]\Big\}\Big\}\Big],\end{aligned}$$

$$A_3=-\left(\frac{1-e^{2kH}}{1+e^{2kH}}\right)ke_{15}(\sigma+\xi)\left[C_0^0k-D_0^0k-\frac{e_{15}}{\varepsilon_{11}}(B_0^0P_1)\right],$$

$$\begin{aligned}A_4=-\xi\Big[&-P_2E_0^0\sigma+2e^{-P_2d}\sigma-B_0^0P_1\sigma-\mu_TE_0^0P_2^2-2P_2\mu_Te^{-P_2d}\\&-(\mu_L-\mu_T)a_1\big[a_1E_0^0P_2^2+2a_1e^{-P_2d}P_2+ika_2E_0^0P_2-2ika_2e^{-P_2d}\big]\\&+i\lambda\Big\{\Big(\mu_TE_0^0+\frac{2}{P_2}\mu_Te^{-P_2d}\Big)(-ik)+(\mu_L-\mu_T)a_2\big[a_1(-P_2E_0^0+2e^{-P_2d})\\&-ika_2\Big(E_0^0+\frac{2}{P_2}e^{-P_2d}\Big)\big]\Big\}\Big],\end{aligned}$$

$$\begin{aligned}A_0^1=\frac{2}{P_2}\overline{c_{44}}P_1&\left(\frac{\sigma-\xi_1}{\sigma+\xi}+\xi_1\right)\frac{e^{-P_2d}}{E^1(k)}-\frac{2}{P_2}\left(\frac{\sigma-\xi_1}{\sigma+\xi}+\xi_1\right)\frac{e_{15}^2}{\varepsilon_{11}}\\&\times k\left(\frac{e^{kH}+e^{-kH}}{e^{kH}-e^{kH}}\right)\tan P_1H\,\frac{e^{-P_2d}}{E^1(k)},\end{aligned}$$

$$\begin{aligned}B_0^1=-\frac{2}{P_2}\frac{\left(\frac{\sigma-\xi_1}{\sigma+\xi}+\xi_1\right)}{E^1(k)}\Bigg[&\bar{c}_{44}P_1-\frac{e_{15}^2}{\varepsilon_{11}}k\left(\frac{e^{kH}}{e^{kH}-e^{-kH}}\right)\sec P_1H\\&+\frac{e_{15}^2}{\varepsilon_{11}}k\left(\frac{e^{kH}+e^{-kH}}{e^{kH}-e^{-kH}}\right)\Bigg]e^{-P_2d},\end{aligned}$$

$$C_0^1=\frac{e_{15}(e^{-kH}\sec P_1H-1)}{\varepsilon_{11}\sec P_1H(e^{kH}-e^{-kH})}A_0^1+\frac{e_{15}\tan P_1H}{\varepsilon_{11}\sec P_1H(e^{kH}-e^{-kH})}B_0^1,$$

$$D_0^1=-\frac{e_{15}(e^{kH}\sec P_1H-1)}{\varepsilon_{11}\sec P_1H(e^{kH}-e^{-kH})}A_0^1-\frac{e_{15}\tan P_1H}{\varepsilon_{11}\sec P_1H(e^{kH}-e^{-kH})}B_0^1,$$

$$E_0^1=-\frac{2}{P_2}\left(\frac{\sigma-\xi_1}{\sigma+\xi}\right)e^{-P_2d}+\frac{\sigma}{\sigma+\xi}A_0^1,$$

$$A_1^1=\frac{R^*(k)\beta_1}{(\sigma+\xi)E^1(k)}-\frac{\beta_2R_2^1(k)e^{-kH}\sec P_1He_{15}k}{E^1(k)}\left(\frac{e^{kH}+e^{-kH}}{e^{kH}-e^{-kH}}\right),$$

$$B_1^1=-\frac{R^*(k)\alpha_1}{(\sigma+\xi)E^1(k)}-\frac{\alpha_2R_2^1(k)e^{-kH}\sec P_1He_{15}k}{E^1(k)}\left(\frac{e^{kH}+e^{-kH}}{e^{kH}-e^{-kH}}\right),$$

$$C_1^1=\frac{R_2^1(k)e^{-kH}}{(e^{-kH}-e^{kH})}-\frac{\frac{e_{15}}{\varepsilon_{11}}(\sec P_1He^{-kH}-1)}{\sec P_1H(e^{-kH}-e^{kH})}A_1^1-\frac{\frac{e_{15}}{\varepsilon_{11}}\tan P_1H}{\sec P_1H(e^{-kH}-e^{kH})}B_1^1,$$

$$D_1^1=\frac{R_2^1(k)e^{kH}}{(e^{kH}-e^{-kH})}-\frac{\frac{e_{15}}{\varepsilon_{11}}(\sec P_1He^{kH}-1)}{\sec P_1H(e^{kH}-e^{-kH})}A_1^1-\frac{\frac{e_{15}}{\varepsilon_{11}}\tan P_1H}{\sec P_1H(e^{kH}-e^{-kH})}B_1^1,$$

$$E_1^1=-\frac{R_1^1(k)}{\sigma+\xi}+\frac{\sigma}{\sigma+\xi}A_1^1,$$

where

$$R^*(k)=R_3^1(k)(\sigma+\xi)+R_2^1(k)e_{15}\left(1-\frac{\beta_2}{\beta_1}\sec P_1He^{-kH}\right)\times\left(\frac{e^{kH}+e^{-kH}}{e^{kH}-e^{-kH}}\right)(\sigma+\xi)-R_1^1(k)\xi.$$

$$\begin{aligned}X=\frac{2}{P_2}\overline{c_{44}}P_1&\left(\frac{\sigma-\xi_1}{\sigma+\xi}+\xi_1\right)(\cot P_1x-1)-\frac{2}{P_2}\left(\frac{\sigma-\xi_1}{\sigma+\xi}+\xi_1\right)\frac{e_{15}^2}{\varepsilon_{11}}\\&\times k\left(\frac{e^{kH}+e^{-kH}}{e^{kH}-e^{kH}}\right)(\cot P_1x\tan P_1H+1)+\frac{2}{P_2}\left(\frac{\sigma-\xi_1}{\sigma+\xi}+\xi_1\right)\frac{e_{15}^2}{\varepsilon_{11}}\\&\times k\left(\frac{e^{kH}}{e^{kH}-e^{-kH}}\right)\sec P_1H,\end{aligned}$$

$$\begin{aligned} Y = {} & \frac{R^*(k)}{(\sigma+\xi)}(\beta_1 \cot P_1 x - \alpha_1) - R_2^1(k)e^{-kH}\sec P_1 H e_{15} \\ & \times k\left(\frac{e^{kH}+e^{-kH}}{e^{kH}-e^{-kH}}\right)(\beta_2 \cot P_1 x + \alpha_2), \end{aligned}$$

$$\begin{aligned} B_2 = {} & \Bigg\{\Big[-c_{44}A_0^1P_1^2 + e_{15}\left(k^2C_0^1 + D_0^1k^2 + \frac{e_{15}}{\varepsilon_{11}}(-A_0^1P_1^2)\right) \\ & -\mu_T P_2^2 E_0^1 - \mu_T 2e^{-P_2 d}P_2 - (\mu_L-\mu_T)a_1\big[a_1(P_2^2E_0^1 + 2e^{-P_2 d}P_2) \\ & - ika_2(-P_2E_0^1 + 2e^{-P_2 d})\big]\Big] + e_{15}\left(1-\frac{\beta_2}{\beta_1}\sec P_1 H e^{-kH}\right) \\ & \times\left(\frac{e^{kH}+e^{-kH}}{e^{kH}-e^{-kH}}\right)\left[C_0^1k - D_0^1k - \frac{e_{15}}{\varepsilon_{11}}(B_0^1P_1)\right]\Bigg\}\beta_1 \cot P_1 x - \alpha_1), \end{aligned}$$

$$\begin{aligned} B_3 = {} & -\xi\left(\frac{\beta_1\cot P_1 x - \alpha_1}{\sigma+\xi}\right)\big[-P_2E_0^1\sigma + 2e^{-P_2 d}\sigma - B_0^1P_1\sigma - \mu_T E_0^1 P_2^2 \\ & - 2P_2\mu_T e^{-P_2 d} - (\mu_L-\mu_T)a_1\big[a_1E_0^1P_2^2 + 2a_1e^{-P_2 d}P_2 \\ & + ika_2E_0^1P_2 - 2ika_2e^{-P_2 d}\big]\big], \end{aligned}$$

$$\begin{aligned} B_4 = {} & -e^{-kH}\sec P_1 H e_{15} k\left(\frac{e^{kH}+e^{-kH}}{e^{kH}-e^{-kH}}\right)(\beta_2\cot P_1 x + \alpha_2) \\ & \times\left[C_0^1k - D_0^1k - \frac{e_{15}}{\varepsilon_{11}}(B_0^1P_1)\right], \end{aligned}$$

Appendix B

$$\begin{aligned} G_1^0 = {} & \overline{c_{44}}\varepsilon_{11}(1+e^{2kH})P_1\Big[k\mu_T + \Gamma_1[\mu_T + (\mu_L-\mu_T)a_1^2]k\sqrt{\frac{s_2^2}{P}-\frac{R^2}{4P^2}} \\ & + \Gamma_2[\mu_T + (\mu_L-\mu_T)a_1^2]\frac{kR}{2P} + \Gamma_2(\mu_L-\mu_T)a_1a_2k\Big], \end{aligned}$$

$$\begin{aligned} G_2^0 = {} & -ke_{15}^2(1-e^{2kH})\Big[k\mu_T + \Gamma_1[\mu_T + (\mu_L-\mu_T)a_1^2]k\sqrt{\frac{s_2^2}{P}-\frac{R^2}{4P^2}} \\ & + \Gamma_2[\mu_T + (\mu_L-\mu_T)a_1^2]\frac{kR}{2P} + \Gamma_2(\mu_L-\mu_T)a_1a_2k\Big] \\ & - k\mu_T[\mu_T + (\mu_L-\mu_T)a_1^2]k\sqrt{\frac{s_2^2}{P}-\frac{R^2}{4P^2}}\varepsilon_{11}(1+e^{2kH}), \end{aligned}$$

$$\begin{aligned} G_3^0 = {} & \overline{c_{44}}\varepsilon_{11}(1+e^{2kH})P_1\Bigg[\frac{\Gamma_1 kR}{2P}[\mu_T + (\mu_L-\mu_T)a_1^2] \\ & - \Gamma_2[\mu_T + (\mu_L-\mu_T)a_1^2]k\sqrt{\frac{s_2^2}{P}-\frac{R^2}{4P^2}} + \Gamma_1(\mu_L-\mu_T)a_1a_2k\Bigg], \end{aligned}$$

$$\begin{aligned} G_4^0 = {} & -ke_{15}^2(1-e^{2kH})\Big[\frac{\Gamma_1 kR}{2P}[\mu_T + (\mu_L-\mu_T)a_1^2] - \Gamma_2[\mu_T + (\mu_L-\mu_T)a_1^2] \\ & \times k\sqrt{\frac{s_2^2}{P}-\frac{R^2}{4P^2}} + \Gamma_1(\mu_L-\mu_T)a_1a_2k\Big] - k\mu_T\varepsilon_{11}(1+e^{2kH}) \\ & \times\Big\{[\mu_T + (\mu_L-\mu_T)a_1^2]\frac{kR}{2P} + (\mu_L-\mu_T)a_1a_2k\Big\}, \end{aligned}$$

$$\begin{aligned} G_1^1 = {} & \overline{c_{44}}\varepsilon_{11}(1-e^{2kH})P_1\Big[k\mu_T + \Gamma_1[\mu_T + (\mu_L-\mu_T)a_1^2]k\sqrt{\frac{s_2^2}{P}-\frac{R^2}{4P^2}} \\ & + \Gamma_2[\mu_T + (\mu_L-\mu_T)a_1^2]\frac{kR}{2P} + \Gamma_2(\mu_L-\mu_T)a_1a_2k\Big], \end{aligned}$$

$$\begin{aligned} G_2^1 = {} & ke_{15}^2(e^{2kH} + 1 - 2\sec P_1 H e^{kH})\Big[k\mu_T + \Gamma_1[\mu_T + (\mu_L-\mu_T)a_1^2] \\ & \times k\sqrt{\frac{s_2^2}{P}-\frac{R^2}{4P^2}} + \Gamma_2[\mu_T + (\mu_L-\mu_T)a_1^2]\frac{kR}{2P} + \Gamma_2(\mu_L-\mu_T)a_1a_2k\Big] \\ & + k\mu_T[\mu_T + (\mu_L-\mu_T)a_1^2]k\sqrt{\frac{s_2^2}{P}-\frac{R^2}{4P^2}}\varepsilon_{11}(1-e^{2kH}), \end{aligned}$$

$$\begin{aligned} G_3^1 = {} & \overline{c_{44}}\varepsilon_{11}(1-e^{2kH})P_1\Bigg[\frac{\Gamma_1 kR}{2P}[\mu_T + (\mu_L-\mu_T)a_1^2] \\ & - \Gamma_2[\mu_T + (\mu_L-\mu_T)a_1^2]k\sqrt{\frac{s_2^2}{P}-\frac{R^2}{4P^2}} + \Gamma_1(\mu_L-\mu_T)a_1a_2k\Bigg], \end{aligned}$$

$$\begin{aligned} G_4^1 = {} & ke_{15}^2(e^{2kH} + 1 - 2\sec P_1 H e^{kH})\Big[\frac{\Gamma_1 kR}{2P}[\mu_T + (\mu_L-\mu_T)a_1^2] \\ & - \Gamma_2[\mu_T + (\mu_L-\mu_T)a_1^2]k\sqrt{\frac{s_2^2}{P}-\frac{R^2}{4P^2}} + \Gamma_1(\mu_L-\mu_T)a_1a_2k\Big] \\ & + k\mu_T\varepsilon_{11}(1-e^{2kH})\Big\{[\mu_T + (\mu_L-\mu_T)a_1^2]\frac{kR}{2P} + (\mu_L-\mu_T)a_1a_2k\Big\}, \end{aligned}$$

$$\begin{aligned} G_5^j = {} & G_1^j\Big[2k\mu_T + 2\mu_T\Gamma_1 k\sqrt{\frac{s_2^2}{P}-\frac{R^2}{4P^2}} \\ & + 2\Gamma_1(\mu_L-\mu_T)a_1^2k\sqrt{\frac{s_2^2}{P}-\frac{R^2}{4P^2}} + \mu_T\Gamma_2\frac{kR}{P} \\ & - \Gamma_2(\mu_L-\mu_T)2ka_1a_2\Big] + G_3^j\Big[\Gamma_2 k\sqrt{\frac{s_2^2}{P}-\frac{R^2}{4P^2}} \\ & + 2\Gamma_2(\mu_L-\mu_T)a_1^2k\sqrt{\frac{s_2^2}{P}-\frac{R^2}{4P^2}}\Big] \end{aligned}$$

(for $j = 0,1$)

$$\begin{aligned} G_6^j = {} & 4k^2\mu_T\varepsilon_{11}(1+e^{2kH})[\mu_T + (\mu_L-\mu_T)a_1^2]k\sqrt{\frac{s_2^2}{P}-\frac{R^2}{4P^2}} \\ & + G_2^j\Big[2k\mu_T + 2\mu_T\Gamma_1 k\sqrt{\frac{s_2^2}{P}-\frac{R^2}{4P^2}} + 2\Gamma_1(\mu_L-\mu_T)a_1^2k\sqrt{\frac{s_2^2}{P}-\frac{R^2}{4P^2}} \\ & + \mu_T\Gamma_2\frac{kR}{P} - \Gamma_2(\mu_L-\mu_T)2ka_1a_2\Big] + G_4^j\Big[\Gamma_2 k\sqrt{\frac{s_2^2}{P}-\frac{R^2}{4P^2}} \\ & + 2\Gamma_2(\mu_L-\mu_T)a_1^2k\sqrt{\frac{s_2^2}{P}-\frac{R^2}{4P^2}}\Big], \end{aligned}$$

$$\begin{aligned} G_7^j = {} & -G_1^j\Big[2\mu_T k\Gamma_2\sqrt{\frac{s_2^2}{P}-\frac{R^2}{4P^2}} + 2\Gamma_2(\mu_L-\mu_T)a_1^2k\sqrt{\frac{s_2^2}{P}-\frac{R^2}{4P^2}} \\ & + 2\mu_T\Gamma_1\frac{kR}{2P} + 2\Gamma_1(\mu_L-\mu_T)a_1^2\frac{kR}{2P} - 2\Gamma_1(\mu_L-\mu_T)a_1a_2k\Big] \\ & + G_3^j\Big[2k\mu_T + 2\mu_T k\Gamma_1\sqrt{\frac{s_2^2}{P}-\frac{R^2}{4P^2}} + 2\Gamma_1(\mu_L-\mu_T)a_1^2k\sqrt{\frac{s_2^2}{P}-\frac{R^2}{4P^2}} \\ & + 2\mu_T\Gamma_2\frac{kR}{2P} + 2\Gamma_2(\mu_L-\mu_T)a_1^2\frac{kR}{2P} - 2a_1a_2k\Gamma_2(\mu_L-\mu_T)\Big], \end{aligned}$$

$$
\begin{aligned}
G_8^j &= 4k^2\mu_T\varepsilon_{11}(1+e^{2kH})[\mu_T+(\mu_L-\mu_T)a_1^2]\frac{kR}{2P}\\
&\quad -G_2^j\Big[2\mu_T k\Gamma_2\sqrt{\frac{s_2^2}{P}-\frac{R^2}{4P^2}}+2\Gamma_2(\mu_L-\mu_T)a_1^2k\sqrt{\frac{s_2^2}{P}-\frac{R^2}{4P^2}}\\
&\quad +2\mu_T\Gamma_1\frac{kR}{2P}+2\Gamma_1(\mu_L-\mu_T)a_1^2\frac{kR}{2P}-2\Gamma_1(\mu_L-\mu_T)a_1a_2k\Big]\\
&\quad +G_4^j\Big[2k\mu_T+2\mu_T k\Gamma_1\sqrt{\frac{s_2^2}{P}-\frac{R^2}{4P^2}}\\
&\quad +2\Gamma_1(\mu_L-\mu_T)a_1^2k\sqrt{\frac{s_2^2}{P}-\frac{R^2}{4P^2}}+2\mu_T\Gamma_2\frac{kR}{2P}\\
&\quad +2\Gamma_2(\mu_L-\mu_T)a_1^2\frac{kR}{2P}-2a_1a_2k\Gamma_2(\mu_L-\mu_T)\Big],
\end{aligned}
$$

$$
\begin{aligned}
G_9^j &= k\mu_T+\Gamma_1[\mu_T+(\mu_L-\mu_T)a_1^2]k\sqrt{\frac{s_2^2}{P}-\frac{R^2}{4P^2}}\\
&\quad +\Gamma_2[\mu_T+(\mu_L-\mu_T)a_1^2]\frac{kR}{2P}+\Gamma_2(\mu_L-\mu_T)a_1a_2k,
\end{aligned}
$$

$$
\begin{aligned}
G_{10}^j &= -\Gamma_2[\mu_T+(\mu_L-\mu_T)a_1^2]k\sqrt{\frac{s_2^2}{P}-\frac{R^2}{4P^2}}\\
&\quad +\Gamma_1[\mu_T+(\mu_L-\mu_T)a_1^2]\frac{kR}{2P}+\Gamma_1(\mu_L-\mu_T)a_1a_2k,
\end{aligned}
$$

$$
\begin{aligned}
G_{11}^j &= -\Big\{G_5^jk\sqrt{\frac{s_2^2}{P}-\frac{R^2}{4P^2}}-G_7^j\frac{kR}{P}\Big\}[\mu_T+(\mu_L-\mu_T)a_1^2]\\
&\quad -2[\mu_T+(\mu_L-\mu_T)a_1^2]\Big[k\sqrt{\frac{s_2^2}{P}-\frac{R^2}{4P^2}}\\
&\quad \times\big\{\Gamma_1(G_9^jG_1^j-G_{10}^jG_3^j)+\Gamma_2(G_9^jG_3^j+G_{10}^jG_1^j)\big\}\\
&\quad -\frac{kR}{P}\big\{\Gamma_1(G_9^jG_3^j+G_{10}^jG_1^j)+\Gamma_2(G_{10}^jG_3^j-G_9^jG_1^j)\big\}\Big]\\
&\quad +(\mu_L-\mu_T)ka_1a_2G_7^j-2(\mu_L-\mu_T)ka_1a_2\big\{\Gamma_1(G_9^jG_3^j+G_{10}^jG_1^j)\\
&\quad +\Gamma_2(G_{10}^jG_3^j-G_9^jG_1^j)\big\},
\end{aligned}
$$

$$
\begin{aligned}
G_{12}^j &= 4k\mu_T\varepsilon_{11}G_9^j\overline{c_{44}}P_1^2(1+e^{2kH})[\mu_T+(\mu_L-\mu_T)a_1^2]\\
&\quad +4k\mu_Te_{15}(1+e^{2kH})k^2G_9^j[\mu_T+(\mu_L-\mu_T)a_1^2]\\
&\quad -\Big\{G_6^jk\sqrt{\frac{s_2^2}{P}-\frac{R^2}{4P^2}}-G_8^j\frac{kR}{P}\Big\}[\mu_T+(\mu_L-\mu_T)a_1^2]\\
&\quad +(\mu_L-\mu_T)ka_1a_2G_8^j-2[\mu_T+(\mu_L-\mu_T)a_1^2]\\
&\quad \times\Big[k\sqrt{\frac{s_2^2}{P}-\frac{R^2}{4P^2}}\big\{\Gamma_1(G_9^jG_2^j-G_{10}^jG_4^j)+\Gamma_2(G_9^jG_4^j+G_{10}^jG_2^j)\big\}\\
&\quad -\frac{kR}{P}\big\{\Gamma_1(G_9^jG_4^j+G_{10}^jG_2^j)+\Gamma_2(G_{10}^jG_4^j-G_9^jG_2^j)\big\}\Big],
\end{aligned}
$$

$$
\begin{aligned}
G_{13}^j &= -\Big\{G_7^jk\sqrt{\frac{s_2^2}{P}-\frac{R^2}{4P^2}}+G_5^j\frac{kR}{P}\Big\}[\mu_T+(\mu_L-\mu_T)a_1^2]\\
&\quad -2[\mu_T+(\mu_L-\mu_T)a_1^2]\Big[k\sqrt{\frac{s_2^2}{P}-\frac{R^2}{4P^2}}\\
&\quad \times\big\{\Gamma_1(G_9^jG_3^j+G_{10}^jG_1^j)-\Gamma_2(G_9^jG_1^j-G_{10}^jG_3^j)\big\}\\
&\quad +\frac{kR}{P}\big\{\Gamma_1(G_9^jG_1^j-G_{10}^jG_3^j)+\Gamma_2(G_9^jG_3^j+G_{10}^jG_1^j)\big\}\Big]\\
&\quad +\frac{kR}{P}\big\{\Gamma_1(G_9^jG_1^j-G_{10}^jG_3^j)+\Gamma_2(G_9^jG_3^j+G_{10}^jG_1^j)\big\}\Big]\\
&\quad -(\mu_L-\mu_T)ka_1a_2G_5^j+2ka_1s_2(\mu_L-\mu_T)\\
&\quad \times\big\{\Gamma_1(G_9^jG_1^j-G_{10}^jG_3^j)+\Gamma_2(G_9^jG_3^j+G_{10}^jG_1^j)\big\}
\end{aligned}
$$

$$
\begin{aligned}
G_{14}^j &= 4k\mu_T\varepsilon_{11}G_{10}^j\overline{c_{44}}P_1^2(1+e^{2kH})[\mu_T+(\mu_L-\mu_T)a_1^2]\\
&\quad +4k\mu_Te_{15}(1+e^{1kH})k^2G_{10}^j[\mu_T+(\mu_L-\mu_T)a_1^2]\\
&\quad -\Big\{G_8^jk\sqrt{\frac{s_2^2}{P}-\frac{R^2}{4P^2}}+G_6^j\frac{kR}{P}\Big\}[\mu_T+(\mu_L-\mu_T)a_1^2]\\
&\quad -2[\mu_T+(\mu_L-\mu_T)a_1^2]\Big[k\sqrt{\frac{s_2^2}{P}-\frac{R^2}{4P^2}}\\
&\quad \times\big\{\Gamma_1(G_9^jG_4^j+G_{10}^jG_2^j)-\Gamma_2(G_9^jG_2^j-G_{10}^jG_4^j)\big\}\\
&\quad +\frac{kR}{P}\big\{\Gamma_1(G_9^jG_2^j-G_{10}^jG_4^j)+\Gamma_2(G_9^jG_4^j+G_{10}^jG_2^j)\big\}\Big]\\
&\quad -(\mu_L-\mu_T)ka_1a_2G_6^j+2(\mu_L-\mu_T)ka_1a_2\\
&\quad \times\big\{\Gamma_1(G_9^jG_2^j-G_{10}^jG_4^j)+\Gamma_2(G_9^jG_4^j+G_{10}^jG_2^j)\big\},
\end{aligned}
$$

$$
G_{15}^j = 4k\mu_T(1-e^{2kH})ke_{15}^2P_1[\mu_T+(\mu_L-\mu_T)a_1^2]G_9^j,
$$

$$
G_{16}^j = -4k\mu_T\frac{1-e^{2kH}}{1+e^{2kH}}k^2e_{15}^2(1-e^{2kH})[\mu_T+(\mu_L-\mu_T)a_1^2]G_9^j,
$$

$$
G_{17}^j = 4k\mu_T(1-e^{2kH})ke_{15}^2P_1[\mu_T+(\mu_L-\mu_T)a_1^2]G_{10}^j,
$$

$$
G_{18}^j = -4k\mu_T\frac{1-e^{2kH}}{1+e^{2kH}}k^2e_{15}^2(1-e^{2kH})[\mu_T+(\mu_L-\mu_T)a_1^2]G_{10}^j,
$$

$$
\begin{aligned}
G_{19}^j &= -k\mu_TG_5^j+2k\mu_T\big\{\Gamma_1(G_9^jG_1^j-G_{10}^jG_3^j)\\
&\quad +\Gamma_2(G_9^jG_3^j+G_{10}^jG_1^j)\big\}-4k\mu_T\varepsilon_{11}G_9^j(1+e^{2kH})\\
&\quad \times[\mu_T+(\mu_L-\mu_T)a_1^2]-[\mu_T+(\mu_L-\mu_T)a_1^2]\\
&\quad \Big\{k\sqrt{\frac{s_2^2}{P}-\frac{R^2}{4P^2}}(\Gamma_1G_5^j-\Gamma_2G_7^j)-\frac{kR}{2P}(\Gamma_1G_7^j-\Gamma_2G_5^j)\Big\}\\
&\quad -2[\mu_T+(\mu_L-\mu_T)a_1^2]\Big[k\sqrt{\frac{s_2^2}{P}-\frac{R^2}{4P^2}}\\
&\quad \times\big\{(\Gamma_1^2-\Gamma_2^2)(G_9^jG_1^j-G_{10}^jG_3^j)+2\Gamma_1\Gamma_2(G_9^jG_3^j+G_{10}^jG_1^j)\big\}\\
&\quad -\frac{kR}{2P}\big\{(\Gamma_1^2-\Gamma_2^2)(G_9^jG_3^j+G_{10}^jG_1^j)-2\Gamma_1\Gamma_2(G_9^jG_1^j-G_{10}^jG_3^j)\big\}\Big]\\
&\quad +(\mu_L-\mu_T)a_1a_2k(G_7^j\Gamma_1-G_5^j\Gamma_2)-2ka_1a_2(\mu_L-\mu_T)\\
&\quad \times\big\{(\Gamma_1^2-\Gamma_2^2)(G_9^jG_3^j+G_{10}^jG_1^j)-2\Gamma_1\Gamma_2(G_9^jG_1^j-G_{10}^jG_3^j)\big\},
\end{aligned}
$$

$$
\begin{aligned}
G_{20}^j &= -k\mu_TG_6+2k\mu_T\big\{\Gamma_1(G_9^jG_2^j-G_{10}^jG_4^j)\\
&\quad +\Gamma_2(G_9^jG_4^j+G_{10}^jG_2^j)\big\}-[\mu_T+(\mu_L-\mu_T)a_1^2]\\
&\quad \times\Big\{k\sqrt{\frac{s_2^2}{P}-\frac{R^2}{4P^2}}(\Gamma_1G_6^j-\Gamma_2G_8^j)-\frac{kR}{2P}(\Gamma_1G_8^j-\Gamma_2G_6^j)\Big\}\\
&\quad -2[\mu_T+(\mu_L-\mu_T)a_1^2]\Big[k\sqrt{\frac{s_2^2}{P}-\frac{R^2}{4P^2}}\\
&\quad \times\big\{(\Gamma_1^2-\Gamma_2^2)(G_9^jG_2^j-G_{10}^jG_4^j)+2\Gamma_1\Gamma_2(G_9^jG_4^j+G_{10}^jG_2^j)\big\}
\end{aligned}
$$

$$-\frac{kR}{2P}\left\{(\Gamma_1^2-\Gamma_2^2)(G_9^jG_4^j+G_{10}^jG_2^j)-2\Gamma_1\Gamma_2(G_9^jG_2^j-G_{10}^jG_4^j)\right\}\Big]$$
$$+(\mu_L-\mu_T)a_1a_2k(G_8^j\Gamma_1-G_6^j\Gamma_2)-2ka_1a_2(\mu_L-\mu_T)$$
$$\times\left\{(\Gamma_1^2-\Gamma_2^2)(G_9^jG_4^j+G_{10}^jG_2^j)-2\Gamma_1\Gamma_2(G_9^jG_2^j-G_{10}^jG_4^j)\right\},$$

$$G_{21}^j=-k\mu_TG_7^j+2k\mu_T\left\{-\Gamma_2(G_9^jG_1^j-G_{10}^jG_3^j)+\Gamma_1(G_9^jG_3^j+G_{10}^jG_1^j)\right\}$$
$$-4k\mu_T\varepsilon_{11}G_{10}^j(1+e^{2kH})[\mu_T+(\mu_L-\mu_T)a_1^2]-[\mu_T+(\mu_L-\mu_T)a_1^2]$$
$$\times\left\{\frac{kR}{2P}(\Gamma_1G_5^j-\Gamma_2G_7^j)+k\sqrt{\frac{s_2^2}{P}-\frac{R^2}{4P^2}}(\Gamma_1G_7^j-\Gamma_2G_5^j)\right\}$$
$$-2[\mu_T+(\mu_L-\mu_T)a_1^2]\Big[\frac{kR}{2P}\left\{(\Gamma_1^2-\Gamma_2^2)(G_9^jG_1^j-G_{10}^jG_3^j)\right.$$
$$\left.+2\Gamma_1\Gamma_2(G_9^jG_3^j+G_{10}^jG_1^j)\right\}+k\sqrt{\frac{s_2^2}{P}-\frac{R^2}{4P^2}}\left\{(\Gamma_1^2-\Gamma_2^2)(G_9^jG_3^j+G_{10}^jG_1^j)\right.$$
$$\left.-2\Gamma_1\Gamma_2(G_9^jG_1^j-G_{10}^jG_3^j)\right\}\Big]+(\mu_L-\mu_T)a_1a_2k(G_5^j\Gamma_1+G_7^j\Gamma_2)$$
$$-2ka_1a_2(\mu_L-\mu_T)\left\{2\Gamma_1\Gamma_2(G_9^jG_3^j+G_{10}^jG_1^j)+(\Gamma_1^2-\Gamma_2^2)(G_9^jG_1^j-G_{10}^jG_3^j)\right\},$$

$$G_{22}^j=-k\mu_TG_8^j+2k\mu_T\left\{-\Gamma_2(G_9^jG_2^j-G_{10}^jG_4^j)+\Gamma_1(G_9^jG_4^j+G_{10}^jG_2^j)\right\}$$
$$-[\mu_T+(\mu_L-\mu_T)a_1^2]$$
$$\times\left\{\frac{kR}{2P}(\Gamma_1G_6^j-\Gamma_2G_8^j)+k\sqrt{\frac{s_2^2}{P}-\frac{R^2}{4P^2}}(\Gamma_1G_8^j-\Gamma_2G_6^j)\right\}$$
$$-2[\mu_T+(\mu_L-\mu_T)a_1^2]$$
$$\times\Big[\frac{kR}{2P}\left\{(\Gamma_1^2-\Gamma_2^2)(G_9^jG_2^j-G_{10}^jG_4^j)+2\Gamma_1\Gamma_2(G_9^jG_4^j+G_{10}^jG_2^j)\right\}$$
$$+k\sqrt{\frac{s_2^2}{P}-\frac{R^2}{4P^2}}\left\{(\Gamma_1^2-\Gamma_2^2)(G_9^jG_4^j+G_{10}^jG_2^j)-2\Gamma_1\Gamma_2(G_9^jG_2^j-G_{10}^jG_4^j)\right\}\Big]$$
$$+(\mu_L-\mu_T)a_1a_2k(G_6^j\Gamma_1+G_8^j\Gamma_2)-2ka_1a_2(\mu_L-\mu_T)$$
$$\times\left\{2\Gamma_1\Gamma_2(G_9^jG_4^j+G_{10}^jG_2^j)+(\Gamma_1^2-\Gamma_2^2)(G_9^jG_2^j-G_{10}^jG_4^j)\right\},$$

$$G_{23}^j=-[\mu_T+(\mu_L-\mu_T)a_1^2]k\sqrt{\frac{s_2^2}{P}-\frac{R^2}{4P^2}}G_{19}^j+\left\{[\mu_T+(\mu_L-\mu_T)a_1^2]\frac{kR}{2P}+(\mu_L-\mu_T)a_1a_2k\right\}G_{21}^j,$$

$$G_{24}^j=-[\mu_T+(\mu_L-\mu_T)a_1^2]k\sqrt{\frac{s_2^2}{P}-\frac{R^2}{4P^2}}G_{20}^j+\left\{[\mu_T+(\mu_L-\mu_T)a_1^2]\frac{kR}{2P}+(\mu_L-\mu_T)a_1a_2k\right\}G_{22}^j,$$

$$G_{25}^j=[\mu_T+(\mu_L-\mu_T)a_1^2]k\sqrt{\frac{s_2^2}{P}-\frac{R^2}{4P^2}}G_{21}^j+\left\{[\mu_T+(\mu_L-\mu_T)a_1^2]\frac{kR}{2P}+(\mu_L-\mu_T)a_1a_2k\right\}G_{19}^j,$$

$$G_{26}^j=[\mu_T+(\mu_L-\mu_T)a_1^2]k\sqrt{\frac{s_2^2}{P}-\frac{R^2}{4P^2}}G_{22}^j+\left\{[\mu_T+(\mu_L-\mu_T)a_1^2]\frac{kR}{2P}+(\mu_L-\mu_T)a_1a_2k\right\}G_{20}^j,$$

$$\chi_1^j=-\Big[G_1^j+\frac{H'}{4[\mu_T+(\mu_L-\mu_T)a_1^2]k\mu_T}(G_{11}^j+G_{15}^j+G_{23}^j)\Big]$$
$$\times\Big[G_2^j+\frac{H'}{4[\mu_T+(\mu_L-\mu_T)a_1^2]k\mu_T}(G_{12}^j+G_{16}^j+G_{24}^j)\Big]$$
$$-\Big[G_3^j+\frac{H'}{4[\mu_T+(\mu_L-\mu_T)a_1^2]k\mu_T}(G_{13}^j+G_{17}^j+G_{25}^j)\Big]$$
$$\times\Big[G_4^j+\frac{H'}{4[\mu_T+(\mu_L-\mu_T)a_1^2]k\mu_T}(G_{14}^j+G_{18}^j+G_{26}^j)\Big],$$

$$\chi_2^j=\left[G_1^j+\frac{H'}{4[\mu_T+(\mu_L-\mu_T)a_1^2]k\mu_T}(G_{11}^j+G_{15}^j+G_{23}^j)\right]^2$$
$$+\left[G_3^j+\frac{H'}{4[\mu_T+(\mu_L-\mu_T)a_1^2]k\mu_T}(G_{13}^j+G_{17}^j+G_{25}^j)\right]^2,$$

$$\chi_3^j=-\left[G_1^j+\frac{H'}{4[\mu_T+(\mu_L-\mu_T)a_1^2]k\mu_T}(G_{11}^j+G_{15}^j+G_{23}^j)\right]$$
$$\times\left[G_4^j+\frac{H'}{4[\mu_T+(\mu_L-\mu_T)a_1^2]k\mu_T}(G_{14}^j+G_{18}^j+G_{26}^j)\right]$$
$$+\left[G_2^j+\frac{H'}{4[\mu_T+(\mu_L-\mu_T)a_1^2]k\mu_T}(G_{12}^j+G_{16}^j+G_{24}^j)\right]$$
$$\times\left[G_3^j+\frac{H'}{4[\mu_T+(\mu_L-\mu_T)a_1^2]k\mu_T}(G_{13}^j+G_{17}^j+G_{25}^j)\right].$$

Appendix C

$$N_1=-\left\{2k\mu_T\overline{c_{44}}\varepsilon_{11}(1+e^{2kH})P_1k\mu_Tk\sqrt{\frac{s_2^2}{P}-\frac{R^2}{4P^2}}\right\}[\mu_T+(\mu_L-\mu_T)a_1^2],$$

$$N_2=4k\mu_T\varepsilon_{11}k\mu_T\overline{c_{44}}P_1^2(1+e^{2kH})[\mu_T+(\mu_L-\mu_T)a_1^2]$$
$$+4k\mu_Te_{15}(1+e^{2kH})k^2k\mu_T[\mu_T+(\mu_L-\mu_T)a_1^2]$$
$$-\Big\{\Big[4k^2\mu_T\varepsilon_{11}(1+e^{2kH})[\mu_T+(\mu_L-\mu_T)a_1^2]k\sqrt{\frac{s_2^2}{P}-\frac{R^2}{4P^2}}$$
$$+2k\mu_T\Big\{-ke_{15}^2(1-e^{2kH})k\mu_T-k\mu_T[\mu_T+(\mu_L-\mu_T)a_1^2]$$
$$\times k\sqrt{\frac{s_2^2}{P}-\frac{R^2}{4P^2}}\varepsilon_{11}(1+e^{2kH})\Big\}\Big]k\sqrt{\frac{s_2^2}{P}-\frac{R^2}{4P^2}}$$
$$-\Big\{4k^2\mu_T\varepsilon_{11}(1+e^{2kH})[\mu_T+(\mu_L-\mu_T)a_1^2]\frac{kR}{2P}$$
$$+2k\mu_T\Big[-k\mu_T\varepsilon_{11}(1+e^{2kH})\Big\{[\mu_T+(\mu_L-\mu_T)a_1^2]\frac{kR}{2P}$$
$$+(\mu_L-\mu_T)a_1a_2k\Big\}\Big]\Big\}\frac{kR}{P}\Big\}[\mu_T+(\mu_L-\mu_T)a_1^2]$$
$$+(\mu_L-\mu_T)ka_1a_2\Big\{4k^2\mu_T\varepsilon_{11}(1+e^{2kH})$$
$$\times[\mu_T+(\mu_L-\mu_T)a_1^2]\frac{kR}{2P}+2k\mu_T\Big[-k\mu_T\varepsilon_{11}(1+e^{2kH})$$
$$\times\Big\{[\mu_T+(\mu_L-\mu_T)a_1^2]\frac{kR}{2P}+(\mu_L-\mu_T)a_1a_2k\Big\}\Big]\Big\},$$

$$N_3=-\left\{2k\mu_T\overline{c_{44}}\varepsilon_{11}(1+e^{2kH})P_1k\mu_T\frac{kR}{P}\right\}[\mu_T+(\mu_L-\mu_T)a_1^2]$$
$$-(\mu_L-\mu_T)ka_1a_2\Big[2k\mu_T\overline{c_{44}}\varepsilon_{11}(1+e^{2kH})P_1k\mu_T\Big],$$

$$N_4=-\Big\{\Big[4k^2\mu_T\varepsilon_{11}(1+e^{2kH})[\mu_T+(\mu_L-\mu_T)a_1^2]\frac{kR}{2P}+$$
$$2k\mu_T\Big[-k\mu_T\varepsilon_{11}(1+e^{2kH})\Big\{[\mu_T+(\mu_L-\mu_T)a_1^2]\frac{kR}{2P}$$

$$+(\mu_L-\mu_T)a_1a_2k\big\}\big]\big]k\sqrt{\frac{s_2^2}{P}-\frac{R^2}{4P^2}}+\big[4k^2\mu_T\varepsilon_{11}(1+e^{2kH})$$

$$[\mu_T+(\mu_L-\mu_T)a_1^2]k\sqrt{\frac{s_2^2}{P}-\frac{R^2}{4P^2}}$$

$$+2k\mu_T\big\{-ke_{15}^2(1-e^{2kH})k\mu_T-k\mu_T$$

$$[\mu_T+(\mu_L-\mu_T)a_1^2]k\sqrt{\frac{s_2^2}{P}-\frac{R^2}{4P^2}}\varepsilon_{11}(1+e^{2kH})\big\}\big]\frac{kR}{P}\Big\}$$

$$\times[\mu_T+(\mu_L-\mu_T)a_1^2]-(\mu_L-\mu_T)ka_1a_2$$

$$\big[4k^2\mu_T\varepsilon_{11}(1+e^{2kH})[\mu_T+(\mu_L-\mu_T)a_1^2]k\sqrt{\frac{s_2^2}{P}-\frac{R^2}{4P^2}}$$

$$+2k\mu_T\big\{-ke_{15}^2(1-e^{2kH})k\mu_T-k\mu_T$$

$$[\mu_T+(\mu_L-\mu_T)a_1^2]k\sqrt{\frac{s_2^2}{P}-\frac{R^2}{4P^2}}\varepsilon_{11}(1+e^{2kH})\big\}\big],$$

$$N_5=4k\mu_T(1-e^{2kH})ke_{15}^2P_1[\mu_T+(\mu_L-\mu_T)a_1^2]k\mu_T,$$

$$N_6=-4k\mu_T\frac{1-e^{2kH}}{1+e^{2kH}}k^2e_{15}^2(1-e^{2kH})[\mu_T+(\mu_L-\mu_T)a_1^2]k\mu_T,$$

$$N_7=-[\mu_T+(\mu_L-\mu_T)a_1^2]k\sqrt{\frac{s_2^2}{P}-\frac{R^2}{4P^2}}\big\{-k\mu_T\big\{2k\mu_T\overline{c_{44}}\varepsilon_{11}(1+e^{2kH})P_1k\mu_T\big\}$$

$$-4k\mu_T\varepsilon_{11}k\mu_T(1+e^{2kH})[\mu_T+(\mu_L-\mu_T)a_1^2]\big\},$$

$$N_8=-[\mu_T+(\mu_L-\mu_T)a_1^2]k\sqrt{\frac{s_2^2}{P}-\frac{R^2}{4P^2}}$$

$$\big[-4k^2\mu_T\varepsilon_{11}k\mu_T(1+e^{2kH})[\mu_T+(\mu_L-\mu_T)a_1^2]k\sqrt{\frac{s_2^2}{P}-\frac{R^2}{4P^2}}$$

$$+2k^2\mu_T^2\big\{-ke_{15}^2(1-e^{2kH})k\mu_T-k\mu_T$$

$$[\mu_T+(\mu_L-\mu_T)a_1^2]k\sqrt{\frac{s_2^2}{P}-\frac{R^2}{4P^2}}\varepsilon_{11}(1+e^{2kH})\big\}\big]$$

$$+\big\{[\mu_T+(\mu_L-\mu_T)a_1^2]\frac{kR}{2P}+(\mu_L-\mu_T)a_1a_2k\big\}$$

$$\big[-k\mu_T\big[4k^2\mu_T\varepsilon_{11}(1+e^{2kH})[\mu_T+(\mu_L-\mu_T)a_1^2]\frac{kR}{2P}$$

$$+2k\mu_T\big[-k\mu_T\varepsilon_{11}(1+e^{2kH})$$

$$\big\{[\mu_T+(\mu_L-\mu_T)a_1^2]\frac{kR}{2P}+(\mu_L-\mu_T)a_1a_2k\big\}\big]\big]\big],$$

$$N_9=\big\{[\mu_T+(\mu_L-\mu_T)a_1^2]\frac{kR}{2P}+(\mu_L-\mu_T)a_1a_2k\big\}$$

$$\big[-k\mu_T\big\{2k\mu_T\overline{c_{44}}\varepsilon_{11}(1+e^{2kH})P_1k\mu_T\big\}$$

$$-4k\mu_T\varepsilon_{11}k\mu_T(1+e^{2kH})[\mu_T+(\mu_L-\mu_T)a_1^2]\big],$$

$$N_{10}=[\mu_T+(\mu_L-\mu_T)a_1^2]k\sqrt{\frac{s_2^2}{P}-\frac{R^2}{4P^2}}\big[-k\mu_T\big[4k^2\mu_T\varepsilon_{11}(1+e^{2kH})$$

$$\times[\mu_T+(\mu_L-\mu_T)a_1^2]\frac{kR}{2P}+2k\mu_T\big[-k\mu_T\varepsilon_{11}(1+e^{2kH})$$

$$\times\big\{[\mu_T+(\mu_L-\mu_T)a_1^2]\frac{kR}{2P}+(\mu_L-\mu_T)a_1a_2k\big\}\big]\big]\big]$$

$$+\big\{[\mu_T+(\mu_L-\mu_T)a_1^2]\frac{kR}{2P}+(\mu_L-\mu_T)a_1a_2k\big\}$$

$$\times\big[-4k^2\mu_T\varepsilon_{11}k\mu_T(1+e^{2kH})[\mu_T+(\mu_L-\mu_T)a_1^2]$$

$$\times k\sqrt{\frac{s_2^2}{P}-\frac{R^2}{4P^2}}+2k^2\mu_T^2\big\{-ke_{15}^2(1-e^{2kH})k\mu_T$$

$$-k\mu_T[\mu_T+(\mu_L-\mu_T)a_1^2]k\sqrt{\frac{s_2^2}{P}-\frac{R^2}{4P^2}}\varepsilon_{11}(1+e^{2kH})\big\}\big],$$

$$\chi_4^0=-\Big[\overline{c_{44}}\varepsilon_{11}(1+e^{2kH})P_1k\mu_T+\frac{H'}{4[\mu_T+(\mu_L-\mu_T)a_1^2]k\mu_T}$$

$$\times(N_1+N_5+N_7)\Big]\big[-ke_{15}^2(1-e^{2kH})k\mu_T$$

$$-k\mu_T[\mu_T+(\mu_L-\mu_T)a_1^2]k\sqrt{\frac{s_2^2}{P}-\frac{R^2}{4P^2}}\varepsilon_{11}(1+e^{2kH})$$

$$+\frac{H'}{4[\mu_T+(\mu_L-\mu_T)a_1^2]k\mu_T}(N_2+N_6+N_8)\big]$$

$$-\Big[\frac{H'}{4[\mu_T+(\mu_L-\mu_T)a_1^2]k\mu_T}(N_3+N_9)\Big]$$

$$\times\big[-k\mu_T\varepsilon_{11}(1+e^{2kH})\big\{[\mu_T+(\mu_L-\mu_T)a_1^2]\frac{kR}{2P}$$

$$+(\mu_L-\mu_T)a_1a_2k\big\}+\frac{H'}{4[\mu_T+(\mu_L-\mu_T)a_1^2]k\mu_T}(N_4+N_{10})\big],$$

$$\chi_5^0=\Big[\overline{c_{44}}\varepsilon_{11}(1+e^{2kH})P_1k\mu_T+\frac{H'}{4[\mu_T+(\mu_L-\mu_T)a_1^2]k\mu_T}$$

$$\times(N_1+N_5+N_7)\Big]+\Big[\frac{H'}{4[\mu_T+(\mu_L-\mu_T)a_1^2]k\mu_T}\times(N_3+N_9)\Big]^2,$$

$$\tilde{N}_1=-\big\{2k\mu_T\overline{c_{44}}\varepsilon_{11}(1-e^{2kH})P_1k\mu_Tk\sqrt{\frac{s_2^2}{P}-\frac{R^2}{4P^2}}\big\}$$

$$\times[\mu_T+(\mu_L-\mu_T)a_1^2],$$

$$\tilde{N}_2=4k\mu_T\varepsilon_{11}k\mu_T\overline{c_{44}}P_1^2(1+e^{2kH})[\mu_T+(\mu_L-\mu_T)a_1^2]$$

$$+4k\mu_Te_{15}(1+e^{2kH})k^2k\mu_T[\mu_T+(\mu_L-\mu_T)a_1^2]$$

$$-\big\{\big[4k^2\mu_T\varepsilon_{11}(1+e^{2kH})[\mu_T+(\mu_L-\mu_T)a_1^2]k\sqrt{\frac{s_2^2}{P}-\frac{R^2}{4P^2}}$$

$$+2k\mu_T\big[-ke_{15}^2(e^{2kH}+1-2\sec P_1He^{kH})k\mu_T$$

$$-k\mu_T[\mu_T+(\mu_L-\mu_T)a_1^2]k\sqrt{\frac{s_2^2}{P}-\frac{R^2}{4P^2}}\varepsilon_{11}(1-e^{2kH})\big]\big]$$

$$\times k\sqrt{\frac{s_2^2}{P}-\frac{R^2}{4P^2}}-\big[4k^2\mu_T\varepsilon_{11}(1+e^{2kH})[\mu_T+(\mu_L-\mu_T)a_1^2]\frac{kR}{2P}$$

$$+2k\mu_T\big[-k\mu_T\varepsilon_{11}(1-e^{2kH})\big\{[\mu_T+(\mu_L-\mu_T)a_1^2]$$

$$\times\frac{kR}{2P}+(\mu_L-\mu_T)a_1a_2k\big\}\big]\big]\frac{kR}{P}\big\}[\mu_T+(\mu_L-\mu_T)a_1^2]$$

$$+(\mu_L-\mu_T)ka_1a_2\big[4k^2\mu_T\varepsilon_{11}(1+e^{2kH})[\mu_T+(\mu_L-\mu_T)a_1^2]\frac{kR}{2P}$$

$$+2k\mu_T\big[-k\mu_T\varepsilon_{11}(1-e^{2kH})\big\{[\mu_T+(\mu_L-\mu_T)a_1^2]\frac{kR}{2P}$$

$$+(\mu_L-\mu_T)a_1a_2k\big\}\big]\big],$$

$$\tilde{N}_3=-\left\{2k\mu_T\overline{c_{44}}\varepsilon_{11}(1-e^{2kH})P_1k\mu_T\frac{kR}{P}\right\}[\mu_T+(\mu_L-\mu_T)a_1^2]$$
$$-(\mu_L-\mu_T)ka_1a_2\left[2k\mu_T\overline{c_{44}}\varepsilon_{11}(1-e^{2kH})P_1k\mu_T\right],$$

$$\tilde{N}_4=-\Big\{\Big[4k^2\mu_T\varepsilon_{11}(1+e^{2kH})[\mu_T+(\mu_L-\mu_T)a_1^2]\frac{kR}{2P}$$
$$+2k\mu_T\Big[-k\mu_T\varepsilon_{11}(1-e^{2kH})\Big\{[\mu_T+(\mu_L-\mu_T)a_1^2]\frac{kR}{2P}$$
$$+(\mu_L-\mu_T)a_1a_2k\Big\}\Big]\Big]k\sqrt{\frac{s_2^2}{P}-\frac{R^2}{4P^2}}+\Big[4k^2\mu_T\varepsilon_{11}(1+e^{2kH})\mu_T$$
$$+(\mu_L-\mu_T)a_1^2]k\sqrt{\frac{s_2^2}{P}-\frac{R^2}{4P^2}}+2k\mu_T\Big[-ke_{15}^2(e^{2kH}+1$$
$$-2\sec P_1He^{kH})k\mu_T-k\mu_T[\mu_T+(\mu_L-\mu_T)a_1^2]k\sqrt{\frac{s_2^2}{P}-\frac{R^2}{4P^2}}$$
$$\times\varepsilon_{11}(1-e^{2kH})\Big]\Big]\frac{kR}{P}\Big\}[\mu_T+(\mu_L-\mu_T)a_1^2]-(\mu_L-\mu_T)ka_1a_2$$
$$\times\Big[4k^2\mu_T\varepsilon_{11}(1+e^{2kH})[\mu_T+(\mu_L-\mu_T)a_1^2]k\sqrt{\frac{s_2^2}{P}-\frac{R^2}{4P^2}}$$
$$+2k\mu_T\Big[-ke_{15}^2(e^{2kH}+1-2\sec P_1He^{kH})k\mu_T$$
$$-k\mu_T[\mu_T+(\mu_L-\mu_T)a_1^2]k\sqrt{\frac{s_2^2}{P}-\frac{R^2}{4P^2}}\varepsilon_{11}(1-e^{2kH})\Big]\Big],$$

$$\tilde{N}_7=-[\mu_T+(\mu_L-\mu_T)a_1^2]k\sqrt{\frac{s_2^2}{P}-\frac{R^2}{4P^2}}$$
$$\times\Big[-k\mu_T\Big\{2k\mu_T\overline{c_{44}}\varepsilon_{11}(1-e^{2kH})P_1k\mu_T\Big\}-4k\mu_T\varepsilon_{11}k\mu_T$$
$$\times(1+e^{2kH})[\mu_T+(\mu_L-\mu_T)a_1^2]\Big],$$

$$\tilde{N}_8=-[\mu_T+(\mu_L-\mu_T)a_1^2]k\sqrt{\frac{s_2^2}{P}-\frac{R^2}{4P^2}}\Big[-k\mu_T\Big[4k^2\mu_T\varepsilon_{11}(1+e^{2kH})$$
$$\times[\mu_T+(\mu_L-\mu_T)a_1^2]k\sqrt{\frac{s_2^2}{P}-\frac{R^2}{4P^2}}$$
$$+2k\mu_T\Big[-ke_{15}^2(e^{2kH}+1-2\sec P_1He^{kH})k\mu_T$$
$$-k\mu_T[\mu_T+(\mu_L-\mu_T)a_1^2]k\sqrt{\frac{s_2^2}{P}-\frac{R^2}{4P^2}}\varepsilon_{11}(1-e^{2kH})\Big]\Big]\Big]$$
$$-k\mu_T\Big\{[\mu_T+(\mu_L-\mu_T)a_1^2]\frac{kR}{2P}+(\mu_L-\mu_T)a_1a_2k\Big\}$$
$$\times\Big[4k^2\mu_T\varepsilon_{11}(1+e^{2kH})[\mu_T+(\mu_L-\mu_T)a_1^2]\frac{kR}{2P}$$
$$+2k\mu_T\Big[-k\mu_T\varepsilon_{11}(1-e^{2kH})\Big\{[\mu_T+(\mu_L-\mu_T)a_1^2]\frac{kR}{2P}$$
$$+(\mu_L-\mu_T)a_1a_2k\Big\}\Big]\Big],$$

$$\tilde{N}_9=\Big\{[\mu_T+(\mu_L-\mu_T)a_1^2]\frac{kR}{2P}+(\mu_L-\mu_T)a_1a_2k\Big\}$$
$$\times\Big[-k\mu_T\Big\{2k\mu_T\overline{c_{44}}\varepsilon_{11}(1-e^{2kH})P_1k\mu_T\Big\}$$
$$-4k\mu_T\varepsilon_{11}k\mu_T(1+e^{2kH})[\mu_T+(\mu_L-\mu_T)a_1^2]\Big],$$

$$\tilde{N}_{10}=-k\mu_T[\mu_T+(\mu_L-\mu_T)a_1^2]k\sqrt{\frac{s_2^2}{P}-\frac{R^2}{4P^2}}\Big[4k^2\mu_T\varepsilon_{11}(1+e^{2kH})$$
$$\times[\mu_T+(\mu_L-\mu_T)a_1^2]\frac{kR}{2P}+2k\mu_T\Big[-k\mu_T\varepsilon_{11}(1-e^{2kH})$$
$$\times\Big\{[\mu_T+(\mu_L-\mu_T)a_1^2]\frac{kR}{2P}+(\mu_L-\mu_T)a_1a_2k\Big\}\Big]\Big]$$
$$+\Big\{[\mu_T+(\mu_L-\mu_T)a_1^2]\frac{kR}{2P}+(\mu_L-\mu_T)a_1a_2k\Big\}$$
$$\times\Big[-k\mu_T\Big[4k^2\mu_T\varepsilon_{11}(1+e^{2kH})[\mu_T+(\mu_L-\mu_T)a_1^2]$$
$$\times k\sqrt{\frac{s_2^2}{P}-\frac{R^2}{4P^2}}+2k\mu_T\Big\{-ke_{15}^2(e^{2kH}+1-2\sec P_1He^{kH})k\mu_T$$
$$-k\mu_T[\mu_T+(\mu_L-\mu_T)a_1^2]k\sqrt{\frac{s_2^2}{P}-\frac{R^2}{4P^2}}\varepsilon_{11}(1-e^{2kH})\Big\}\Big]\Big],$$

$$\chi_4^1=-\Big[\overline{c_{44}}\varepsilon_{11}(1-e^{2kH})P_1k\mu_T+\frac{H'}{4[\mu_T+(\mu_L-\mu_T)a_1^2]k\mu_T}$$
$$\times(\tilde{N}_1+N_5+\tilde{N}_7)\Big]\Big[\Big\{-ke_{15}^2(e^{2kH}+1-2\sec P_1He^{kH})k\mu_T$$
$$-k\mu_T[\mu_T+(\mu_L-\mu_T)a_1^2]k\sqrt{\frac{s_2^2}{P}-\frac{R^2}{4P^2}}\varepsilon_{11}(1-e^{2kH})\Big\}$$
$$+\frac{H'}{4[\mu_T+(\mu_L-\mu_T)a_1^2]k\mu_T}(\tilde{N}_2+N_6+\tilde{N}_8)\Big]$$
$$-\Big[\frac{H'}{4[\mu_T+(\mu_L-\mu_T)a_1^2]k\mu_T}(\tilde{N}_3+\tilde{N}_9)\Big]$$
$$\times\Big[-k\mu_T\varepsilon_{11}(1-e^{2kH})\Big\{[\mu_T+(\mu_L-\mu_T)a_1^2]\frac{kR}{2P}$$
$$+(\mu_L-\mu_T)a_1a_2k\Big\}+\frac{H'}{4[\mu_T+(\mu_L-\mu_T)a_1^2]k\mu_T}(\tilde{N}_4+\tilde{N}_{10})\Big],$$

$$\chi_5^1=\left[\overline{c_{44}}\varepsilon_{11}(1-e^{2kH})P_1k\mu_T+\frac{H'}{4[\mu_T+(\mu_L-\mu_T)a_1^2]k\mu_T}\right.$$
$$\left.\times(\tilde{N}_1+N_5+\tilde{N}_7)\right]^2+\left[\frac{H'}{4[\mu_T+(\mu_L-\mu_T)a_1^2]k\mu_T}(\tilde{N}_3+\tilde{N}_9)\right]^2.$$